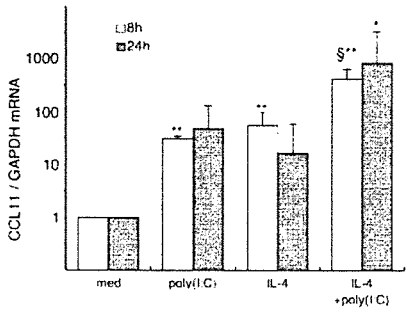

FIGURE 2. *CCL11* mRNA levels adjusted by the amount of *GAPDH* mRNA in BSMC stimulated for 8 or 24 h with 10 μg/ml poly(I:C), 10 ng/ml IL-4, or both combined. *CCL11/GAPDH* mRNA levels in unstimulated BSMC are defined as 1. Mean ± SEM from four experiments using BSMC from different donors. *, $p < 0.05$; **, $p < 0.001$ compared with unstimulated cells. §, $p < 0.05$ compared with IL-4-stimulated cells.

lower chamber was determined by incubating the plate for 10 min with substrate solution (0.5 mM *o*-phenylenediamine, 1 mM H_2O_2, and 0.1% Triton X-100 in Tris buffer (pH 8.0)), followed by the addition of 4 M H_2SO_4 to stop the reaction, and the absorbance was measured at 490 nm.

Flow cytometric analysis of the expression of TLR3

BEAS2B cells or BSMC were resuspended in a concentration of 10^7 cells/ml in PBS containing 0.5% BSA and 20 mM EDTA; incubated for 1 h at 4°C with 1 μg/100 μl anti-human TLR3 Ab (TLR3.7) (22) or 1 μg/100 μl control mouse IgG1 (R&D Systems); washed twice in PBS; and incubated with FITC-labeled anti-mouse IgG $F(ab')_2$ (DakoCytomation) for 1 h at 4°C. A fraction of cells was prefixed with 2% paraformaldehyde in PBS (15 min, 37°C) and permealized with 0.1% saponin in PBS (15 min, 37°C) before the staining to examine the intracellular expression of TLR3. The labeled cells were analyzed using a FACScan flow cytometer (BD Biosciences).

Immunolocalization of TLR3 and poly(I:C) in BSMC by confocal laser-scanning microscopy

Poly(I:C) was labeled with fluorescein using a FastTag FL Kit (Vector Laboratories), according to the manufacturer's instructions. BSMC cultured on glass coverslips coated with poly(L-lysine) were incubated with poly(I:C) for 5 min at 37°C, fixed with 4% paraformaldehyde, and permeabilized with 0.1% saponin at room temperature. Fluorescein-labeled poly(I:C) was stained by serial incubation with an image-iT FX signal enhancer (Molecular Probes), 20 μg/ml Alexa Fluor 488-conjugated rabbit anti-fluorescein IgG (Molecular Probes), and 20 μg/ml Alexa Fluor 488-conjugated goat anti-rabbit IgG (Molecular Probes) at room temperature. In another experiment, early endosome Ag 1 (EEA-1) in endosomes was stained with anti-EEA-1 Ab (10 μg/ml; GeneTex), followed by Alexa Fluor 488-conjugated goat anti-rabbit IgG. After two washes with PBS, the cells were incubated for 1 h at room temperature with 20 μg/ml anti-human TLR3 Ab, or with control mouse IgG1 in 2% BSA/PBS, and washed with PBS. A total of 10 μg/ml Alexa Fluor 568-conjugated rabbit anti-mouse IgG (Molecular Probes) and 10 μg/ml Alexa Fluor 568-conjugated goat anti-rabbit IgG (Molecular Probes) was applied consecutively, followed by incubation with 1 μM TO-PRO3 (Molecular Probes). The cells were then examined by confocal laser-scanning microscopy (LSM510; Zeiss).

Transfection of TLR3 small interfering RNA (siRNA) in BSMC

BSMC were cultured in 24-well plates at a density of 2.5×10^4 cells/well overnight. TLR3 siRNA (5′-GGUUGGUAACGAUUCCUUUGC-3′) or randomly scrambled negative control siRNA was mixed with liposome (Lipofectamine 2000; Invitrogen Life Technologies), according to the manufacurer's instructions, and added to the culture medium containing FBS and growth factors. The cells were washed twice with PBS 72 h later, then stimulated for 3 h with FBS/growth factor-free medium containing either 10 ng/ml IL-4 only or 10 μg/ml IL-4 plus poly(I:C). Total RNA was extracted, and quantitative RT-PCR was performed to determine the levels of *CCL11*, *TLR3*, and *TLR4* mRNA.

Statistical analysis

Data are presented as means ± SEM. Chemokine concentrations in the supernatant, mRNA levels, and eosinophil chemotactic activities were tested with ANOVA, followed by Bonferroni/Dunn procedure as a post hoc test (STATVIEW 1992-98; SAS Institute). Dose-response relationships and kinetics of *CCL11* release were analyzed with repeated-measures ANOVA. A p value <0.05 was considered significant.

Results

A prominent release of *CCL5* from BSMC was induced by 0.1–10 μg/ml poly(I:C), for 24 h ($p < 0.005$), similar to the release of *CCL5* from BEAS2B, a respiratory epithelial cell line (Fig. 1*A*). There was also a significant increase in the release of IL-6, CXCL8, and CXCL10 in BSMC stimulated with 10 μg/ml poly(I:C), compared with those in unstimulated cells (IL-6, 141 ± 102 in unstimulated cells vs 1570 ± 578 pg/ml in poly(I:C)-stimulated cells, $p < 0.01$, $n = 5$; CXCL8, 148 ± 58 vs 1383 ± 408 pg/ml, $p < 0.005$, $n = 6$; CXCL10, 3 ± 2 vs 2598 ± 631 pg/ml, $p < 0.001$, $n = 6$). IL-4 had no synergistic effects on the production of these cytokines and chemokines (Fig. 1*A* and data not shown).

CCL11 was also released from BSMC stimulated with poly(I:C) ($p < 0.05$), but not from BEAS2B (Fig. 1*B*). In presence of 10 ng/ml IL-4, the poly(I:C)-induced release of *CCL11* from BSMC was further increased ($p < 0.05$) compared with poly(I:C) alone (Fig. 1*B*). A total of 0.1–10 μg/ml poly(I:C) also induced the release of *CCL11* in presence of 10 ng/ml IL-13 in a concentration-dependent fashion ($p < 0.005$, data not shown). The kinetics of *CCL11* release from BSMC are shown in Fig. 1*C*. Neither ssRNA, polycystidic acid, nor dsDNA, polydeoxyinosinic-deoxycystidic acid, up to a concentration of 100 μg/ml, increased the IL-4-induced release of CCL11 from BSMC (IL-4 alone, 404 ± 273

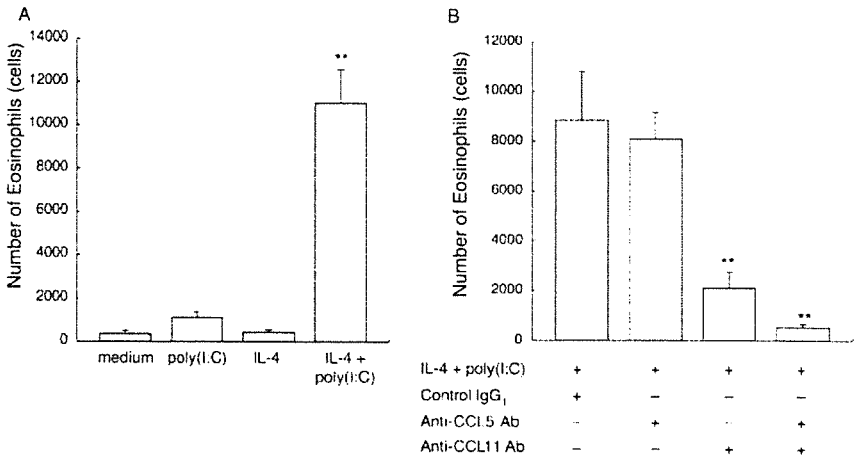

FIGURE 3. *A*, Eosinophil chemotactic activity in the supernatant from BSMC stimulated with 10 μg/ml poly(I:C), 10 ng/ml IL-4, or the combination for 24 h. Mean ± SEM from four duplicate experiments. **, $p < 0.001$. *B*, Neutralization of eosinophil chemotactic activity with anti-chemokine Abs. The supernatant from BSMC stimulated with 10 μg/ml poly(I:C) and 10 ng/ml IL-4, for 24 h, was preincubated with an anti-CCL11 Ab, an anti-CCL5 Ab, or mouse IgG1 (control IgG1). Mean ± SEM from four duplicate experiments. **, $p < 0.005$.

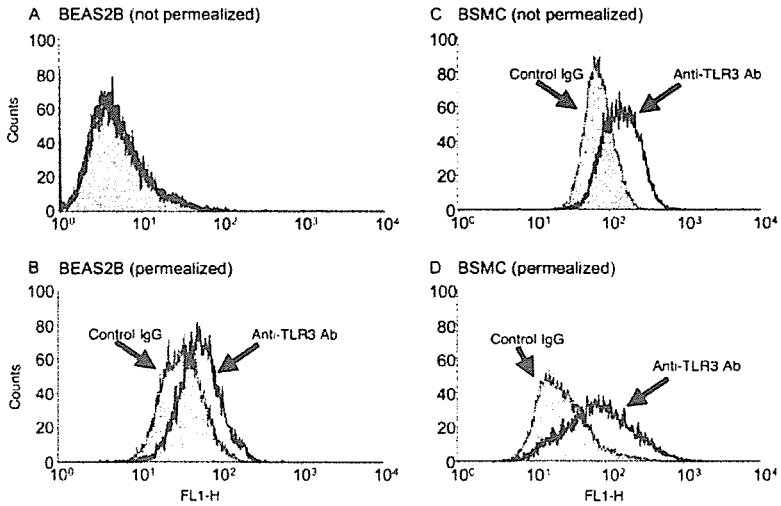

FIGURE 4. Flow cytometric analysis of TLR3 expression in BEAS2B cells (*A* and *B*) and BSMC (*C* and *D*). The cells not permeabilized (*A* and *C*) or permeabilized (*B* and *D*) with 0.1% saponin were incubated with an anti-TLR3 Ab or control mouse IgG, followed by a fluorescein-labeled anti-mouse IgG Ab. Representative data from two to three separate experiments.

pg/ml; IL-4 plus polycystidic acid, 469 ± 380 pg/ml; IL-4 + polydeoxyinosinic-deoxycystidic acid, 598 ± 522 pg/ml, $n = 3$). Preincubation of poly(I:C) for 1 h at 37°C with 10 μg/ml polymyxin B did not modify the release of CCL11 from BSMC (data not shown), excluding an effect of LPS. Quantitative RT-PCR revealed that incubation for 8–24 h with either 10 ng/ml IL-4 or 10 μg/ml poly(I:C) increased the concentrations of *CCL11* mRNA in BSMC significantly ($p < 0.001$), and their combination synergistically enhanced the expression of *CCL11* mRNA ($p < 0.05$; Fig. 2).

Because both CCL5 and CCL11 are potent chemoattractants of eosinophils, we examined whether the culture supernatant of stimulated BSMC exhibited a functional eosinophil chemotactic activity and, if it did, which chemokine was responsible for chemotaxis. The culture supernatant from BSMC stimulated with 10 μg/ml poly(I:C) alone or 10 ng/ml IL-4 alone did not exhibit a significant increase in chemotactic activity for eosinophils compared with the supernatant from unstimulated BSMC (Fig. 3*A*). In contrast, the supernatant from BSMC costimulated with poly(I:C) and IL-4 revealed a significantly increased chemotactic activity ($p < 0.001$). Preincubation of the supernatant with an anti-CCL11 Ab decreased the poly(I:C)/IL-4-induced eosinophil chemotactic activity by >85% ($p < 0.005$, Fig. 3*B*), whereas the preincubation with an anti-CCL5 Ab did not significantly inhibit eosinophil chemotaxis. This suggests that CCL11 is the major chemoattractant for eosinophils released from BSMC stimulated with poly(I:C) and IL-4.

Next, we studied the expression of the dsRNA receptor, TLR3, in BSMC by two approaches. RT-PCR showed the constitutive expression of *TLR3* mRNA in the BSMC as well as BEAS2B (data not shown). Flow cytometric analysis also showed the presence of TLR3 immunoreactivity on the cellular surface of BSMC (Fig. 4*C*), in sharp contrast with BEAS2B cells, in which TLR3 immunoreactivity was detectable only when they were permeabilized with saponin (Fig. 4, *A* and *B*).

To determine the role of TLR3 in the poly(I:C)-induced synthesis of CCL11 in BSMC, 10 μg/ml anti-TLR3-neutralizing Ab was added to the culture medium 1 h before stimulation with poly(I:C) and IL-4. We observed no effect of the anti-TLR3-neutralizing Ab on the release of CCL11 from IL-4/poly(I:C)-stimulated BSMC (Fig. 5*A*). In contrast, bafilomycin A1, an endosome acidification inhibitor, prominently inhibited the release of CCL11 from BSMC stimulated with IL-4 plus poly(I:C) ($p < 0.01$, Fig. 5*B*). Bafilomycin A1 had no effects on the CCL11 release induced by IL-4 alone, suggesting that the acidification of endosomes is needed for the action of poly(I:C). This suggests that the poly(I:C)-induced CCL11 release is not mediated via TLR3 on the cell surface, but via intracellular receptors.

We confirmed by confocal laser-scanning microscopy that TLR3 and exogenously administered poly(I:C) were present inside BSMC. Although, in unstimulated BSMC, the immunoreactivity of TLR3 was distributed throughout the cytoplasm, we observed a strong intracellular aggregation of TLR3 immunoreactivity 5 min after stimulation with poly(I:C) (Fig. 6*A*). Fluorescein-labeled poly(I:C) was also observed in the cytoplasm, and colocalized with TLR3 immunoreactivity (Fig. 6*B*). TLR3 immunoreactivity in poly(I:C)-stimulated BSMC was also colocalized with EEA-1, an endosomal marker (Fig. 6*C*).

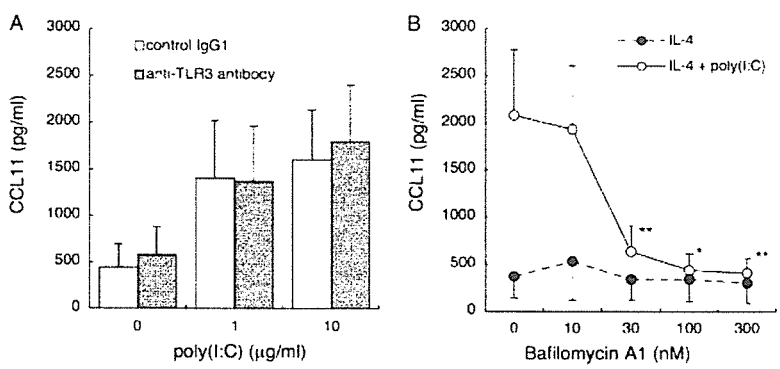

FIGURE 5. *A*, Effects of an anti-TLR3-neutralizing Ab on poly(I:C)/IL-4-induced release of CCL11 from BSMC. Anti-TLR3-neutralizing Ab or control mouse IgG1 was added 1 h before the 24-h stimulation with 10 μg/ml poly(I:C) and 10 ng/ml IL-4. Mean ± SEM from three duplicate experiments, using BSMC from different donors. *B*, Effects of bafilomycin A1 on IL-4-induced or poly(I:C)/IL-4-induced release of CCL11 from BSMC. Bafilomycin A1 inhibited the release of CCL11 from BSMC stimulated with the combination of 10 ng/ml IL-4 and 10 μg/ml poly(I:C), but not with IL-4 alone. Mean ± SEM from the experiments using BSMC from four different donors. *, $p < 0.05$; **, $p < 0.01$ compared with the cells untreated with bafilomycin A1.

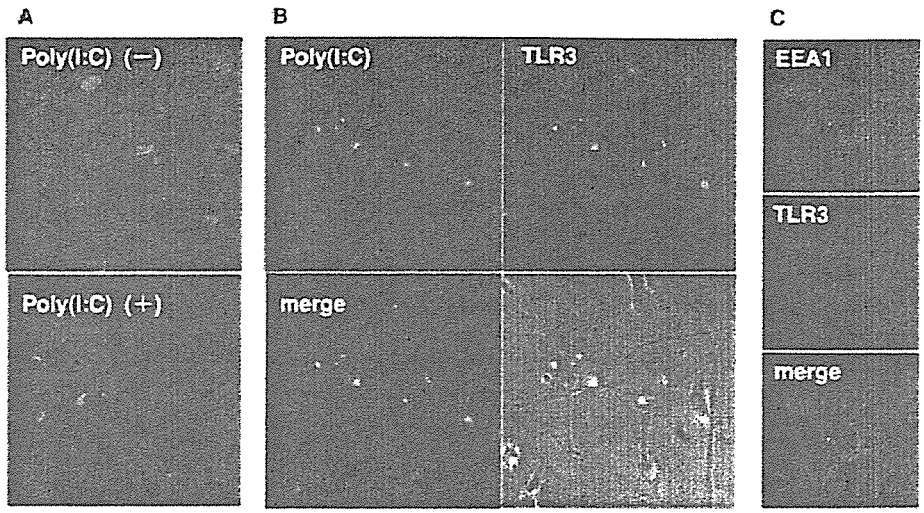

FIGURE 6. Immunolocalization of TLR3 and poly(I:C) in BSMC by confocal laser-scanning microscopy. *A*, TLR3 immunoreactivity (red) in unstimulated and poly(I:C)-stimulated BSMC (10 μg/ml, for 5 min). *B*, Coaggregation of TLR3 (red) and poly(I:C) (green) in poly(I:C)-stimulated BSMC (10 μg/ml, for 5 min). *C*, Coaggregation of TLR3 (red) and EEA-1 (green), an endosomal marker, in poly(I:C)-stimulated BSMC (10 μg/ml, for 5 min). Representative data from three separate experiments.

Finally, we examined the effects of TLR3 siRNA on the poly(I:C)-induced *CCL11* mRNA expression in BSMC. Compared with liposome alone or negative control siRNA, 20 nM TLR3-specific siRNA suppressed the expression of *TLR3* mRNA by >80% (n = 5; $p < 0.01$), but did not change *TLR4* mRNA expression (Fig. 7*A*). A total of 10 μg/ml poly(I:C), in presence of negative control siRNA, increased the expression of *CCL11* mRNA in IL-4-treated BSMC by 4.7 ± 1.1-fold. In contrast, the increase in the expression of *CCL11* was only 1.7 ± 0.2-fold in presence of TLR3 siRNA, significantly less than in presence of negative control siRNA (n = 5; $p < 0.05$; Fig. 7*B*).

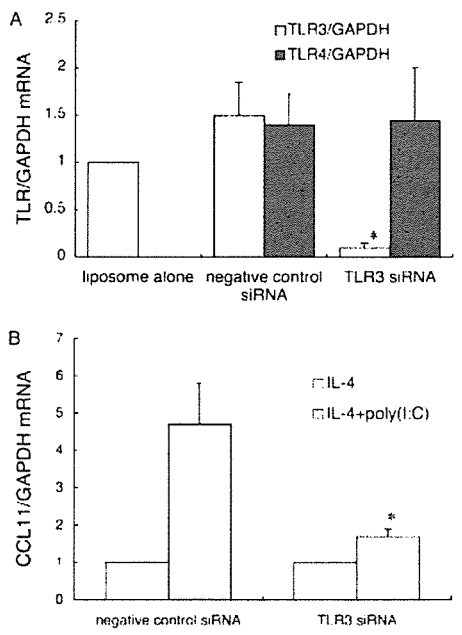

FIGURE 7. Effects of TLR3 siRNA on gene expression in BSMC. *A*, Effects on the expression of *TLR3* and *TLR4* mRNA expression. TLR3 siRNA specifically suppressed the expression of *TLR3* mRNA. Mean ± SEM from five duplicate experiments, using BSMC from different donors. *, $p < 0.05$ compared with negative control siRNA. *B*, Effects on the expression of poly(I:C)-induced *CCL11* mRNA expression. BSMC was stimulated with 10 ng/ml IL-4, or with the combination of 10 μg/ml IL-4 and poly(I:C). *CCL11* mRNA levels in BSMC stimulated with IL-4 alone are presented as 1. Mean ± SEM from five duplicate experiments, using BSMC from different donors. *, $p < 0.05$ compared with negative control siRNA.

Discussion

We have shown that synthetic dsRNA, poly(I:C), and the Th2 cytokine, IL-4, synergistically induced the release of vigorous eosinophil chemotactic activity from primary cultures of human BSMC, an effect mostly mediated by the CC chemokine, CCL11. We have also shown that the activation of intracellular TLR3, a receptor for dsRNA, was required for the poly(I:C)-mediated induction of CCL11 synthesis in BSMC.

A synergism between a Th2-dominant microenvironment and RNA virus infections on the increase in eosinophilia in the airways has been suggested from the results of experiments in vivo (6, 29), although the exact mechanism has not been determined. Previous studies have shown that poly(I:C) or virus-derived dsRNA increases the production of cytokines and chemokines, including IL-6, CCL5, CXCL8, and CXCL10 in primary cultures or immortalized bronchial epithelial cells, such as BEAS2B (15–20). In the present study, we have confirmed that poly(I:C) is also a potent stimulant of the synthesis of CCL5 in BSMC, as well as of IL-6, CXCL8, and CXCL10. The most significant difference observed between BSMC and BEAS2B cells was the production of important amounts of CCL11 by BSMC in presence of IL-4, whereas BEAS2B cells did not produce CCL11, regardless of the presence of IL-4. Synergism between poly(I:C) and Th2 cytokines is also observed in other cell types, including bronchial epithelial cells; it has been reported that poly(I:C) induced eotaxin-3/CCL26 synthesis in BEAS2B cells in the presence of IL-4 (20). More importantly, CCL11, but not CCL5, mediated most of the eosinophil chemotactic activity in the culture supernatant of the poly(I:C)/IL-4-stimulated BSMC. These observations suggest that, in the Th2-dominant microenvironment, respiratory virus infections can exacerbate the eosinophilic inflammation of the airways via the production of CCL11, as observed in a proportion of patients with RSV infections (5).

It has been reported recently that RSV infection in mice with a TLR3 deletion results in increased eosinophil accumulation in the airway accompanied by an increase in pulmonary IL-5 and IL-13 expression (30). We have also observed that poly(I:C) administered simultaneously with aerosolized allergen attenuated airway eosinophilia in sensitized rats, accompanied by an increase in

IFN-γ and IL-12 and a decrease in IL-13 in bronchoalveolar lavage fluid. In contrast, poly(I:C) administered in rats 16 h after allergen exposure, at the time when Th2 responses have already been established, significantly increased the number of eosinophils in bronchoalveolar lavage fluid (Y. Shiraishi, K. Asano, K. Niimi, K. Fukunaga, M. Wakaki, J. Kagyo, T. Takihara, T. Nakajima, T. Oguma, Y, Suzuki, T. Shiomi, K. Sayama, E. Ikeda, H. Hirai, M. Nakamura, and A. Ishizaka, manuscript in preparation). These findings as well as the results of the present study suggest that the activation of TLR3 exacerbates the pre-existed Th2-dependent eosinophilic airway inflammation, although it undermines the development of Th2 responses.

Although the major cellular target for the respiratory RNA virus are the upper and lower respiratory epithelial cells, rhinovirus, RSV, or parainfluenza virus can infect primary cultures of respiratory or gastrointestinal smooth muscle cells directly, and modulate various cellular functions (31–33). For example, the administration of poly(I:C) or RSV infection in colonic smooth muscle cells promoted the adhesion of leukocytes on these cells (33). During the revision of this manuscript, Oliver et al. (34) reported that rhinovirus can infect and replicate in nonasthmatic and asthmatic BSMCs, and induced the expression of IL-6 and CXCL8. Viral infection might also have damaged the infected epithelial cells, causing the leak of virus-derived dsRNA that stimulates surrounding cells, including smooth muscle cells. Epithelial cells in the airways of asthmatics can release even larger amounts of viral RNA than epithelial cells from normal airways, because the impaired synthesis of IFN-β in asthmatic epithelial cells allows a greater viral replication and cellular necrosis (not apoptosis) accompanied by membrane disruption (35). It is further supported by the recent finding that the leakage of rhinovirus-derived RNA into the blood during upper respiratory rhinovirus infections is more prominent in asthmatics than nonasthmatics (36). Besides viral RNA, cellular mRNA leaked from, or associated with, necrotic cells is also capable of activating TLR3 with its secondary structures that contain double-stranded sequences (37).

The subcellular localization of TLR3 differs markedly among various cell types. Its expression is limited to the intracellular compartment in dendritic and mast cells (21, 23), whereas, in fibroblasts, it is expressed on the cell surface, and can be blocked with an anti-TLR3 Ab (22). The localization of TLR3 in respiratory epithelial cells remains controversial. By flow cytometric analysis, its immunoreactivity is limited to the intracellular space, as in dendritic and mast cells, although the anti-TLR3 Ab can partially inhibit the synthesis of poly(I:C)-induced cytokine (38, 39). Although we were able to confirm the expression of TLR3 immunoreactivity on the surface of BSMC by flow cytometric analysis, the anti-TLR3-neutralizing Ab failed to suppress the synthesis of CCL11 in poly(I:C)-stimulated BSMC in the concentration that successfully blocked the synthesis of IFN in poly(I:C)-stimulated fibroblasts (22). This suggests that poly(I:C) is recognized in BSMC by intracellular TLR3 or other cytoplasmic dsRNA receptors, such as protein kinase R or retinoic acid-inducible gene-I (15, 40). Because bafilomycin A1, a vacuolar H^+-ATPase inhibitor, inhibits the acidification of endosome and suppresses the intracelluar uptake of poly(I:C) (41), the suppression of the synthesis of CCL11 in poly(I:C)-stimulated BSMC by treatment with bafilomycin A1 further confirmed the interaction between intracellular receptor(s) and poly(I:C).

We next examined whether TLR3 mediates the poly(I:C)-induced synthesis of CCL11 in BSMC. Although TLR3 mediates the cellular response to RSV and influenza virus in the respiratory epithelial cells and fibroblasts (38, 39, 42), other cytoplasmic receptors for dsRNA, such as protein kinase R and retinoic acid-inducible gene-I, play a major role in different situations (15, 40). First, we showed that poly(I:C) was coaggregated with TLR3 intracellularly, which is possibly located in endosomes. The inhibitory effects of bafilomycin A1 suggest that the endosomes are the site of interaction between poly(I:C) and TLR3. A recent analysis using TLR3-CD32 chimeric receptors has also suggested that an acidic pH, observed in endosomes and phagolysosomes, is necessary for the multimerization and signaling of TLR3 (43). Second, we have shown that targeting the expression of TLR3 with a TLR3-specific siRNA prominently decreased the poly(I:C)-induced mRNA expression of *CCL11* in BSMC. Therefore, we have concluded that the poly(I:C)-induced synthesis of CCL11 in BSMC is mediated, at least partially, by intracellular TLR3.

In conclusion, our observations suggest that BSMC participate in the pathogenesis of exacerbation of inflammation during respiratory viral infections in asthmatic patients. The cellular tropism of the virus, extent of damage in infected epithelial cells, and the airway microenvironment are the main factors that determine the type and intensity of inflammation.

Acknowledgments

We thank Jeffery M. Drazen for reviewing the manuscript, and Miyuki Yamamoto for her expert technical assistance.

Disclosures

The authors have no financial conflict of interest.

References

1. Johnston, S. L., P. K. Pattemore, G. Sanderson, S. Smith, F. Lampe, L. Josephs, P. Symington, S. O'Toole, S. H. Myint, D. A. Tyrrell, et al. 1995. Community study of role of viral infections in exacerbations of asthma in 9–11 year old children. *Br. Med. J.* 310: 1225–1229.
2. Nicholson, K. G., J. Kent, and D. C. Ireland. 1993. Respiratory viruses and exacerbations of asthma in adults. *Br. Med. J.* 307: 982–986.
3. Grunberg, K., H. H. Smits, M. C. Timmers, E. P. de Klerk, R. J. Dolhain, E. C. Dick, P. S. Hiemstra, and P. J. Sterk. 1997. Experimental rhinovirus 16 infection: effects on cell differentials and soluble markers in sputum in asthmatic subjects. *Am. J. Respir. Crit. Care Med.* 156: 609–616.
4. Garofalo, R., J. L. Kimpen, R. C. Welliver, and P. L. Ogra. 1992. Eosinophil degranulation in the respiratory tract during naturally acquired respiratory syncytial virus infection. *J. Pediatr.* 120: 28–32.
5. Kim, C. K., S. W. Kim, C. S. Park, B. I. Kim, H. Kang, and Y. Y. Koh. 2003. Bronchoalveolar lavage cytokine profiles in acute asthma and acute bronchiolitis. *J. Allergy Clin. Immunol.* 112: 64–71.
6. Makela, M. J., R. Tripp, A. Dakhama, J. W. Park, T. Ikemura, A. Joetham, M. Waris, L. J. Anderson, and E. W. Gelfand. 2003. Prior airway exposure to allergen increases virus-induced airway hyperresponsiveness. *J. Allergy Clin. Immunol.* 112: 861–869.
7. Schwarze, J., E. Hamelmann, K. L. Bradley, K. Takeda, and E. W. Gelfand. 1997. Respiratory syncytial virus infection results in airway hyperresponsiveness and enhanced airway sensitization to allergen. *J. Clin. Invest.* 100: 226–233.
8. Becker, S., W. Reed, F. W. Henderson, and T. L. Noah. 1997. RSV infection of human airway epithelial cells causes production of the β-chemokine RANTES. *Am. J. Physiol.* 272: L512–L520.
9. Matsukura, S., F. Kokubu, H. Noda, H. Tokunaga, and M. Adachi. 1996. Expression of IL-6, IL-8, and RANTES on human bronchial epithelial cells, NCI-H292, induced by influenza virus A. *J. Allergy Clin. Immunol.* 98: 1080–1087.
10. Papadopoulos, N. G., A. Papi, J. Meyer, L. A. Stanciu, S. Salvi, S. T. Holgate, and S. L. Johnston. 2001. Rhinovirus infection up-regulates eotaxin and eotaxin-2 expression in bronchial epithelial cells. *Clin. Exp. Allergy* 31: 1060–1066.
11. Schroth, M. K., E. Grimm, P. Frindt, D. M. Galagan, S. I. Konno, R. Love, and J. E. Gern. 1999. Rhinovirus replication causes RANTES production in primary bronchial epithelial cells. *Am. J. Respir. Cell Mol. Biol.* 20: 1220–1228.
12. Matthews, S. P., J. S. Tregoning, A. J. Coyle, T. Hussell, and P. J. Openshaw. 2005. Role of CCL11 in eosinophilic lung disease during respiratory syncytial virus infection. *J. Virol.* 79: 2050–2057.
13. Power, U. F., T. Huss, V. Michaud, H. Plotnicky-Gilquin, J. Y. Bonnefoy, and T. N. Nguyen. 2001. Differential histopathology and chemokine gene expression in lung tissues following respiratory syncytial virus (RSV) challenge of formalin-inactivated RSV- or BBG2Na-immunized mice. *J. Virol.* 75: 12421–12430.
14. Alexopoulou, L., A. C. Holt, R. Medzhitov, and R. A. Flavell. 2001. Recognition of double-stranded RNA and activation of NF-κB by Toll-like receptor 3. *Nature* 413: 732–738.
15. Gern, J. E., D. A. French, K. A. Grindle, R. A. Brockman-Schneider, S. Konno, and W. W. Busse. 2003. Double-stranded RNA induces the synthesis of specific chemokines by bronchial epithelial cells. *Am. J. Respir. Cell Mol. Biol.* 28: 731–737.

16. Ieki, K., S. Matsukura, F. Kokubu, T. Kimura, H. Kuga, M. Kawaguchi, M. Odaka, S. Suzuki, S. Watanabe, H. Takeuchi, et al. 2004. Double-stranded RNA activates RANTES gene transcription through cooperation of nuclear factor-κB and interferon regulatory factors in human airway epithelial cells. *Clin. Exp. Allergy* 34: 745–752.
17. Sha, Q., A. Q. Truong-Tran, J. R. Plitt, L. A. Beck, and R. P. Schleimer. 2004. Activation of airway epithelial cells by Toll-like receptor agonists. *Am. J. Respir. Cell Mol. Biol.* 31: 358–364.
18. Spurrell, J. C., S. Wiehler, R. S. Zaheer, S. P. Sanders, and D. Proud. 2005. Human airway epithelial cells produce IP-10 (CXCL10) in vitro and in vivo upon rhinovirus infection. *Am. J. Physiol.* 289: L85–L95.
19. Taima, K., S. Takanashi, K. Okumura, T. Imaizumi, M. Kumagai, A. Ishikawa, H. Yoshida, K. Satoh, and T. Fujita. 2005. Double-stranded RNA stimulates the expression of monocyte chemoattractant protein-1 in BEAS-2B bronchial epithelial cells. *Exp. Lung Res.* 31: 361–375.
20. Tsuji, K., S. Yamamoto, W. Ou, N. Nishi, I. Kobayashi, M. Zaitsu, E. Muro, Y. Sadakane, T. Ichimaru, and Y. Hamasaki. 2005. dsRNA enhances eotaxin-3 production through interleukin-4 receptor up-regulation in airway epithelial cells. *Eur. Respir. J.* 26: 795–803.
21. Matsumoto, M., K. Funami, M. Tanabe, H. Oshiumi, M. Shingai, Y. Seto, A. Yamamoto, and T. Seya. 2003. Subcellular localization of Toll-like receptor 3 in human dendritic cells. *J. Immunol.* 171: 3154–3162.
22. Matsumoto, M., S. Kikkawa, M. Kohase, K. Miyake, and T. Seya. 2002. Establishment of a monoclonal antibody against human Toll-like receptor 3 that blocks double-stranded RNA-mediated signaling. *Biochem. Biophys. Res. Commun.* 293: 1364–1369.
23. Matsushima, H., N. Yamada, H. Matsue, and S. Shimada. 2004. TLR3-, TLR7-, and TLR9-mediated production of proinflammatory cytokines and chemokines from murine connective tissue type skin-derived mast cells but not from bone marrow-derived mast cells. *J. Immunol.* 173: 531–541.
24. Chung, K. F., H. J. Patel, E. J. Fadlon, J. Rousell, E. B. Haddad, P. J. Jose, J. Mitchell, and M. Belvisi. 1999. Induction of eotaxin expression and release from human airway smooth muscle cells by IL-1β and TNFα: effects of IL-10 and corticosteroids. *Br. J. Pharmacol.* 127: 1145–1150.
25. Ghaffar, O., Q. Hamid, P. M. Renzi, Z. Allakhverdi, S. Molet, J. C. Hogg, S. A. Shore, A. D. Luster, and B. Lamkhioued. 1999. Constitutive and cytokine-stimulated expression of eotaxin by human airway smooth muscle cells. *Am. J. Respir. Crit. Care Med.* 159: 1933–1942.
26. John, M., S. J. Hirst, P. J. Jose, A. Robichaud, N. Berkman, C. Witt, C. H. Twort, P. J. Barnes, and K. F. Chung. 1997. Human airway smooth muscle cells express and release RANTES in response to T helper 1 cytokines: regulation by T helper 2 cytokines and corticosteroids. *J. Immunol.* 158: 1841–1847.
27. Powell, W. S., S. Gravel, F. Halwani, C. S. Hii, Z. H. Huang, A. M. Tan, and A. Ferrante. 1997. Effects of 5-oxo-6,8,11,14-eicosatetraenoic acid on expression of CD11b, actin polymerization, and adherence in human neutrophils. *J. Immunol.* 159: 2952–2959.
28. Nagata, M., K. Saito, K. Tsuchiya, and Y. Sakamoto. 2002. Leukotriene D_4 up-regulates eosinophil adhesion via the cysteinyl leukotriene 1 receptor. *J. Allergy Clin. Immunol.* 109: 676–680.
29. Barends, M., M. Van Oosten, C. G. De Rond, J. A. Dormans, A. D. Osterhaus, H. J. Neijens, and T. G. Kimman. 2004. Timing of infection and prior immunization with respiratory syncytial virus (RSV) in RSV-enhanced allergic inflammation. *J. Infect. Dis.* 189: 1866–1872.
30. Rudd, B. D., J. J. Smit, R. A. Flavell, L. Alexopoulou, M. A. Schaller, A. Gruber, A. A. Berlin, and N. W. Lukacs. 2006. Deletion of TLR3 alters the pulmonary immune environment and mucus production during respiratory syncytial virus infection. *J. Immunol.* 176: 1937–1942.
31. Elias, J. A., Y. Wu, T. Zheng, and R. Panettieri. 1997. Cytokine- and virus-stimulated airway smooth muscle cells produce IL-11 and other IL-6-type cytokines. *Am. J. Physiol.* 273: L648–L655.
32. Hakonarson, H., N. Maskeri, C. Carter, R. L. Hodinka, D. Campbell, and M. M. Grunstein. 1998. Mechanism of rhinovirus-induced changes in airway smooth muscle responsiveness. *J. Clin. Invest.* 102: 1732–1741.
33. de La Motte, C. A., V. C. Hascall, A. Calabro, B. Yen-Lieberman, and S. A. Strong. 1999. Mononuclear leukocytes preferentially bind via CD44 to hyaluronan on human intestinal mucosal smooth muscle cells after virus infection or treatment with poly(I·C). *J. Biol. Chem.* 274: 30747–30755.
34. Oliver, B. G., S. L. Johnston, M. Baraket, J. K. Burgess, N. J. King, M. Roth, S. Lim, and J. L. Black. 2006. Increased proinflammatory responses from asthmatic human airway smooth muscle cells in response to rhinovirus infection. *Respir. Res.* 7: 71.
35. Wark, P. A., S. L. Johnston, F. Bucchieri, R. Powell, S. Puddicombe, V. Laza-Stanca, S. T. Holgate, and D. E. Davies. 2005. Asthmatic bronchial epithelial cells have a deficient innate immune response to infection with rhinovirus. *J. Exp. Med.* 201: 937–947.
36. Xatzipsalti, M., S. Kyrana, M. Tsolia, S. Psarras, A. Bossios, V. Laza-Stanca, S. L. Johnston, and N. G. Papadopoulos. 2005. Rhinovirus viremia in children with respiratory infections. *Am. J. Respir. Crit. Care Med.* 172: 1037–1040.
37. Kariko, K., H. Ni, J. Capodici, M. Lamphier, and D. Weissman. 2004. mRNA is an endogenous ligand for Toll-like receptor 3. *J. Biol. Chem.* 279: 12542–12550.
38. Guillot, L., R. Le Goffic, S. Bloch, N. Escriou, S. Akira, M. Chignard, and M. Si-Tahar. 2005. Involvement of Toll-like receptor 3 in the immune response of lung epithelial cells to double-stranded RNA and influenza A virus. *J. Biol. Chem.* 280: 5571–5580.
39. Hewson, C. A., A. Jardine, M. R. Edwards, V. Laza-Stanca, and S. L. Johnston. 2005. Toll-like receptor 3 is induced by and mediates antiviral activity against rhinovirus infection of human bronchial epithelial cells. *J. Virol.* 79: 12273–12279.
40. Yoneyama, M., M. Kikuchi, T. Natsukawa, N. Shinobu, T. Imaizumi, M. Miyagishi, K. Taira, S. Akira, and T. Fujita. 2004. The RNA helicase RIG-I has an essential function in double-stranded RNA-induced innate antiviral responses. *Nat. Immunol.* 5: 730–737.
41. Vijay-Kumar, M., J. R. Gentsch, W. J. Kaiser, N. Borregaard, M. K. Offermann, A. S. Neish, and A. T. Gewirtz. 2005. Protein kinase R mediates intestinal epithelial gene remodeling in response to double-stranded RNA and live rotavirus. *J. Immunol.* 174: 6322–6331.
42. Rudd, B. D., E. Burstein, C. S. Duckett, X. Li, and N. W. Lukacs. 2005. Differential role for TLR3 in respiratory syncytial virus-induced chemokine expression. *J. Virol.* 79: 3350–3357.
43. De Bouteiller, O., E. Merck, U. A. Hasan, S. Hubac, B. Benguigui, G. Trinchieri, E. E. Bates, and C. Caux. 2005. Recognition of double-stranded RNA by human Toll-like receptor 3 and downstream receptor signaling requires multimerization and an acidic pH. *J. Biol. Chem.* 280: 38133–38145.

Lamprey TLRs with Properties Distinct from Those of the Variable Lymphocyte Receptors[1]

Akihiro Ishii,* Aya Matsuo,* Hirofumi Sawa,† Tadayuki Tsujita,[2]* Kyoko Shida,‡ Misako Matsumoto,*‡ and Tsukasa Seya[3]*‡

Fish express mammalian-type (M-type) TLRs consisting of leucine-rich repeats (LRRs) and Toll-IL-1R (TIR) homology domain for immunity, whereas invertebrates in deuterostomes appear to have no orthologs of M-type TLRs. *Lampetra japonica* (lamprey) belongs to the lowest class of vertebrates with little information about its TLRs. We have identified two cDNA sequences of putative TLRs in the lamprey (laTLRs) that contain LRRs and TIR domains. The two laTLRs were 56% homologous to each other, and their TIRs were similar to those of members of the human TLR2 subfamily, most likely orthologs of fish TLR14. We named them laTLR14a and laTLR14b. We raised a rabbit polyclonal Ab against laTLR14b and identified a 85-kDa protein in a human HEK293 transfectant by immunoblotting using the Ab. FACS, histochemical, and confocal analyses showed that laTLR14b is expressed intracellularly in lamprey gill cells and that the overexpressed protein resides in the endoplasmic reticulum of human and fish (medaka) cell lines. Because natural agonists of TLR14 remained unidentified, we made a chimera construct of extracellular CD4 and the cytoplasmic domain of laTLR14. The chimera molecule of laTLR14b, when expressed in HEK293 cells, elicited activation of NF-κB and, consequently, weak activation of the IFN-β promoter. laTLR14b mRNA was observed in various organs and leukocytes. This lamprey species expressed a variable lymphocyte receptor structurally independent of laTLR14 in leukocytes. Thus, the jawless vertebrate lamprey possesses two LRR-based recognition systems, the variable lymphocyte receptor and TLR, and the M-type TLRs are conserved across humans, fish, and lampreys. *The Journal of Immunology,* 2007, 178: 397–406.

The first line of host defense against pathogen invasion is assigned by the innate immune system. This system involves a number of microbe pattern recognition receptors such as complement receptors, lectins, and TLRs. TLRs have recently been identified as the main receptors for the recognition of microbe-specific pattern molecules (1). TLRs structurally consist of extracytoplasmic leucine-rich repeats (LRRs)[4] and an intracytoplasmic Toll-IL-1R (TIR) homology domain (2–4), similar to *Drosophila* Toll (5). The LRRs sense microbes and the TIR transmits a signal for infectious response. The results of vertebrate and invertebrate genome projects have suggested that the TLR pattern recognition system is conserved across mammalian groups and probably most vertebrate species (6). In contrast, some invertebrates, based on their genomes, have only a few TLR-like proteins, whereas others have >100 members of the TLR family that are structurally unlinked to those of mammals (7). Toll homologues in insects and worms are often related to developmental functions rather than immunity (7, 8). In deuterostomes, based on their genome information invertebrates harbor TLR-like proteins with no homology to human TLRs (huTLRs), whereas gnathostomes, including fishes, amphibians, reptiles, birds, and mammals, have orthologs of huTLRs (6), which we designated the mammalian-type (M-type) TLR system (9). It is becoming clear that M-type TLR family members are mostly related to microbial pattern recognition for immunity (10). Thus, species-specific development of TLR expansion appears to have independently occurred in each division of insects, deuterostome invertebrates, and jawed vertebrates, most of which happen to have a TLR repertoire consisting of multiple members of Toll or TLRs with differential functions (7, 8). It remains unclear whether jawless vertebrates possess the TLR system comparable to that in humans.

Jawed vertebrates generate a lymphocyte receptor repertoire of sufficient diversity to discriminate the antigenic component of any pathogen (11–13). In jawed vertebrates including mammals, lymphocytes recognize peptides mounted on APCs to induce clonal lymphocyte proliferation and activate effector cells, leading to elimination of the pathogen. The initiation of these adaptive immune responses is triggered by the preceding activation of TLR signaling in the APCs. The Ig domains are used for the molecular interactions in the acquired immune system in jawed vertebrates. In contrast, the surviving jawless fish (agnathans), lamprey and hagfish, have diverse lymphocyte Ag receptor genes encoding LRRs (12–14). These cell surface receptors are designated variable lymphocyte receptors (VLRs) (12). VLRs are GPI-anchored proteins retained on the cell surface

*Department of Microbiology and Immunology, Graduate School of Medicine, Hokkaido University, Sapporo, Japan; †Department of Pathology, Zoonosis Center, Hokkaido University, Sapporo Japan; and ‡Department of Immunology, Osaka Medical Center for Cancer and Cardiovascular Diseases, Osaka, Japan

Received for publication February 16, 2006. Accepted for publication October 17, 2006.

The costs of publication of this article were defrayed in part by the payment of page charges. This article must therefore be hereby marked *advertisement* in accordance with 18 U.S.C. Section 1734 solely to indicate this fact.

[1] This work was supported in part by Core Research for Engineering, Science and Technology, Japan Science and Technology Corporation and by Grants-in-Aid from the Ministry of Education, Science and Culture (Specified Project for Advanced Research) of Japan and by the Mitsubishi Foundation (to T.S.), the Takeda Foundation (to T.S.), and the Uehara Memorial Foundation (to M.M.).

[2] Current address: Exploratory Research for Advanced Technology, Japan Science and Technology Corporation, Laboratory of Molecular and Developmental Biology, University of Tsukuba, Tennoudai 1-1-1, Tsukuba 305-8577, Japan.

[3] Address correspondence and reprint requests to Dr. Tsukasa Seya, Department of Microbiology and Immunology, Graduate School of Medicine, Hokkaido University, Kita-ku, Sapporo 060-8638, Japan. E-mail address: seya-tu@pop.med.hokudai.ac.jp

[4] Abbreviations used in this paper: LRR, leucine-rich repeat; ER, endoplasmic reticulum; fgTLR, fugu TLR; huTLR, human TLR; laTLR, lamprey TLR; M-type, mammalian-type; poly(I:C), polyinosinic-polycytidylic acid; TIR, Toll/IL-1R (homology domain); TICAM, TIR domain-containing adaptor molecule; VLR, variable lymphocyte receptor.

membranes or released in the fluid phase like Abs (7). Although the Ag-presenting mechanism, including the machinery for Ag presentation, has not been elucidated in agnathans, recombinatorial mechanisms for the generation of anticipatory receptors thus evolved in both jawless and jawed vertebrates (7). However, the role of innate immunity in the triggering of the VLR response has not been elucidated.

In humans and mice, the TLR system with a multigene family has been characterized as a functional entity specifically recognizing microbial pattern molecules independently of the acquired system (15, 16). To investigate whether jawless fish possesses the TLR family with a functional profile similar to that in humans, we used *Lampetra japonica* (lamprey) to analyze the TLR system. We searched lamprey tissues and cDNA libraries for fish TLR orthologs and found that the lamprey harbors two isoforms of the TLR2 subfamily. One of them resides inside lamprey cells and serves to deliver signals to activate NF-κB and, to a lesser extent, type I IFN in human cells. These results together with their subcellular localization profiles in human and fish cells suggest that the lamprey expresses immune-related TLR orthologs independently of the VLR system.

Materials and Methods

Lampreys

Live lampreys were purchased from Ebetsu Gyokyo. Sectioned tissues of the lamprey were stored at −80°C until use. Whole blood of the lamprey was drained from the dorsal aorta using a syringe, immediately added to an equal volume of Percoll (Amersham Biosciences), and then centrifuged at 2000 rpm for 10 min at 4°C, and the buffy coat was harvested to prepare leukocytes as previously described (17).

Because the chromosomes in jawless fish cells are unstable (18), no cell line is yet available. In addition, jawless fish genome information is difficult to obtain. For these reasons, we used human and fish (medaka, *Oryzias latipes*) cells instead of lamprey cells for the analysis of lamprey proteins. Although the data have been only partially published, the signal pathways of fish TLRs can be principally reconciled in human cells (19).

Cloning of lamprey TLRs (laTLRs) and construction of their constitutive active forms

laTLR DNA fragments were amplified by PCR with degenerated primers from a cDNA library of lamprey embryo mRNA as previously described (20). The primers were designed on the basis of the conserved TIR domain of 200-bp regions of fugu TLR (fgTLR) 1, huTLR1, huTLR6, and huTLR10. 3′- and 5′-RACE followed by consecutive PCR allowed us to identify two distinct sequences of laTLR-like products. The expected sizes of the two cDNA fragments were obtained by the PCR (data not shown). Full-length cDNAs were extended by consecutive PCR and then the two distinct cDNAs of laTLRs were cloned into pEFBOS vector (named laTLR14a and laTLR14b; GenBank accession nos. AB109402 and AB109403, respectively). A FLAG tag was attached to the C terminus of the protein in this vector. N-terminal FLAG-tagged laTLR14b was constructed in a pCMV-FLAG vector (Sigma-Aldrich) as described previously (21).

To analyze the signaling pathway of the laTLRs, TIR domains of laTLR14 (TIR14a and TIR14b) were fused with the human CD4 extracellular domain and cloned into the pEFBOS vector as constitutive active forms (1, 22). Each DNA fragment was amplified by PCR, and the obtained products were digested by *Xho*I and *Bgl*II (CD4), *Bgl*II and *Not*I (TIR14a), and *Bam*HI and *Not*I (TIR14b). The digested DNA fragments of the TIR and the CD4 fragment were cloned into the pEFBOS vector. Sequences of the primers used are shown in Table I.

Abs, cells, and proteins

Anti-human CD4 Ab was purchased from BD Biosciences. Anti-FLAG mAb was purchased from Sigma-Aldrich.

Human HEK293 HeLa cells were obtained from the American Type Culture Collection. RK13 cells (derived from rabbit kidney) were obtained from the RIKEN Cell Bank. HEK293 and RK13 cells were cultured in DMEM containing 10% heat-inactivated FCS. The HeLa cells were cultured in MEM with 2 mM L-glutamine and 10% FCS. These cells were transfected with expression vectors. The medaka fish cell line OL-17 (23) was a gift from Dr. H. Mitani (Tokyo University, Tokyo, Japan). Cells were cultured in L15 medium containing 10 mM HEPES buffer (pH 7.5) with 20% FCS at 33°C.

Rabbit anti-laTLR14b polyclonal Ab was produced by the method established in our laboratory (24). Briefly, RK13 cells (1×10^7) were transiently transfected with a pFLAG CMV-His×6 with full-length laTLR14b construct using LipofectAMINE PLUS reagent (Invitrogen Life Technologies). After 48 h, transfected RK13 cells were collected in 10 mM EDTA-PBS, washed three times with PBS, and suspended in 0.5 ml of PBS. The RK13 cell suspensions were then mixed and emulsified with 0.6 ml of Freund's complete adjuvant (Difco) and used for the immunization of rabbits. Immunization was performed four times at 7-day intervals, and the rabbits were boosted 3 days before drawing blood. Titers of the anti-laTLR14b Ab were roughly estimated by immunoblotting with lines of cell lysate containing laTLR14b (data not shown). IgG was purified by precipitation with 33% ammonium sulfate, dialyzed against PBS, and stored at −80°C until use.

Reporter assay

HEK293 cells (1×10^6 cells/well) were transiently transfected in 6-well plates by using LipofectAMINE 2000 reagent (Invitrogen Life Technologies) with reporter plasmid p-125 luc (IFN-β promoter) or luciferase-linked E-selectin (ELAM) promoter (NF-κB, 1 μg) and an internal control vector (phRL-TK, 0.2 ng; Promega). The total amount of DNA used for transfection was kept constant at 4 μg by adding an empty vector. After 24 h, cells were harvested and added to 96-well plates (5×10^4 cells/well) and stimulated with PBS, 10 μg/ml *Staphylococcus aureus* peptidoglycan (Furuka-Chemie), 100 nM macrophage-activating lipopeptide-2 (Biologica), 100 ng/ml Pam3 (BioLinks), 100 ng/ml LPS (Difco), 10 μg/ml polyinosinic-polycytidylic acid (poly(I:C); Amersham Biosciences), 1 μg/ml *Vibrio anguillarum* flagellin (19), and 1/100 volume of sonicated *Clostridium sporogenes* and *Salmonella typhimurium* cell lysates (25). After 6 h, cells were lysed in lysis buffer (Promega) and assayed for firefly and *Renilla* luciferase activities. Firefly luciferase activity was normalized with that of *Renilla* and expressed as fold stimulation relative to the activity of vector-transfected cells or PBS-stimulated cells. In some experiments, HEK293 cells (2×10^5 cells/well) in 24-well plates were transfected with pEFBOS/human CD4-laTLR14b plasmid (0.2 μg), the reporter plasmid (0.2 μg), internal control vector (0.1 ng), and the indicated expression vectors with dominant negative adapters (0.4 μg). After 12 h, cells were lysed and assayed for reporter activity. The SD was calculated from three separate experiments, each performed in triplicate.

RNA preparation and RT-PCR analysis

Individual female lampreys were dissected and the skin, gills, heart, liver, gut (stomach and intestine), kidneys, muscle, eyes, and eggs were harvested. A section above the vertebral column (called marrow) was aspirated with a syringe. One hundred milligrams of each tissue was homogenized in 1 ml of TRIzol reagent (Invitrogen Life Technologies) using a Dounce-type glass homogenizer and then total RNA was extracted by the TRIzol RNA preparation method. Five hundred nanograms of total RNA was treated with RQ1 RNase-free DNase and reverse transcribed with Moloney murine leukemia virus reverse transcriptase and random primers. For amplification of laTLR14 fragments, PCR was performed by denaturation at 94°C for 5 min followed by 35 cycles of 94°C for 30 s, 60°C for 30 s, and extension at 72°C for 30 s. *L. japonica* VLR DNA fragments were also amplified similarly for 30 cycles. Ex-*Taq* polymerase (Takara) and the indicated primers were used for both reactions (Table I).

Gene analysis

Assembling and editing of the determined DNA sequences were performed with ATGC and GENETYX-MAC version 12.1 software (Software Development). The sequences of the predicted open reading frames and TIR domains were compared with other sequences in a homology search by the BLAST program (www.ncbi.nlm.nih.gov/BLAST/). TLR14 members of *Takifugu rubripes* (GenBank accession nos. AC156431 and AAW69369), *Danio rerio* (GenBank accession no. XP_687315), and *Xenopus tropicalis* (Department of Energy Joint Genome Institute identifiers 190020, 30694, 421728, and 421736) were identified in the BLAST database. Alignment of amino acid sequences and unrooted phylogenic analysis of TLRs were performed using the ClustalW program (www.ddbj.nig.ac.jp/search/clustalw-j.html). Functional domains of the proteins were predicted by the SMART program (http://smart.embl-heidelberg.de/).

Flow cytometry and immunoblotting

Transfected HEK293 cells were analyzed for protein expression by flow cytometry and immunoblotting. For flow cytometric analysis, cells were

Table I. *Primers used in this study*[a]

Name	Sequence	Object
TLR16101	GANTGGTGCCAYTAYGGAR	Lamprey TLR cloning
TLR101R1	GCNCKNARGTTGGGCCARAA	Lamprey TLR cloning
TLRb85FW	TTTGCGGCCGCGAAAAAATGTTGCTGCGGAGAC	Construction for FLAG-tagged TLRb
TLRb2469RVS	TTTGTCGACTTTAAACATAAGGGTTACGGATTG	Construction for FLAG-tagged TLRb
CA_CD4FW	TTTCTCGAGCCCACAATGAACCGGGGAGTCCC	Construction for constitutive active form
CA_CD4RVS	TTTAGATCTCACCGGGGTGGACC	Construction for constitutive active form
CA_TIRaFW	TTTGAGATCTGCGATCGGACTC	Construction for constitutive active form
CA_TIRaRVS	TTTGCGGCCGCTTACTTGTCATCGTCGTC	Construction for constitutive active form
CA_TIRbFW	TTTGGATCCATCTCCATGAGCGTTGGAA	Construction for constitutive active form
CA_TIRbRVS	TTTGCGGCCGCTTAAACATAAGGGTTACGG	Construction for constitutive active form
RTa-500FW	TCCTTGAGAGAGCTGTATCTGACG	RT-PCR
RTa-RVS	AGTCCGAGTCCATGTGGCTGTAGG	RT-PCR
RTb-1000FW	GATTTTCCACGTACCCATGACGTACC	RT-PCR
RTb-500FW	TACATTGCACCCGAGTTGTACTCC	RT-PCR
RTb-RVS	GTGGGCACCAGGGTGTTCTCCACC	RT-PCR
Actin-FW	TGCTACGTGGCGCTCGACTTCGAG	RT-PCR
Actin-RVS	CCTTCTGCATGCGGTCGGCGATGC	RT-PCR
VLR-FW	CCTGGTGCAAAGTGCGGTAG	RT-PCR
VLR-RVS	CGGACGGGGGTATTGGTACCAG	RT-PCR

[a] FW, Forward; RVS, reverse.

stained with anti-TLR14b Ab (250-fold diluted in PBS with 0.2% BSA) or anti-FLAG Ab (5 μg/ml), washed in PBS containing 0.2% BSA and 0.1% sodium azide, and then incubated with FITC-conjugated goat anti-mouse IgG (American Qualex). Cells were washed and fluorescence intensity was measured (FACSCalibur; BD Biosciences). For immunoblotting, various lamprey tissues were solubilized in lysis buffer (1% (v/v) Nonidet P-40, 0.14 M NaCl, 0.01 M EDTA, 0.02 M Tris-HCl (pH 7.4), 1 mg/ml iodoacetamide, and 1 mM PMSF) using a Dounce-type homogenizer. After incubation at 4°C for 30 min, each lysate was centrifuged at 15,000 rpm for 30 min at 4°C. The supernatants were collected and protein concentration was measured using a protein estimation kit (Bio-Rad). Equal amounts of total cellular protein from each lysate were resolved by SDS-PAGE (7.5% gel) and transferred to polyvinylidene difluoride membranes. The membranes were incubated with either anti-laTLR14b Ab (1,000-fold diluted in PBS with 0.02% Nonidet P-40) or anti-FLAG Ab (5 μg/ml), washed in PBS containing 0.02% Nonidet P-40, and tagged by HRP-linked goat anti-rabbit second Ab (BioSource International). Proteins reacting to the Ab were visualized using an ECL detection system (Amersham Bioscience).

Confocal microscope analysis

HeLa cells or OL-17 cells of the Hd-rR strain of medaka (23) (1.5×10^5 cells/well) were plated onto coverslips in a 24-well plate. Cells were then transiently transfected with vectors expressing FLAG-tagged proteins. At timed intervals, the adherent cells were fixed for 30 min with 3% formaldehyde in PBS and permeabilized with 0.5% saponin in 1% BSA and PBS for 30 min and then washed four times with PBS. After the cells had been soaked in 1% BSA and PBS, they were treated for 1 h at room temperature with 5 μg/ml mouse anti-FLAG Ab (Sigma-Aldrich). The cells were then washed with 1% BSA and PBS and treated for 30 min at room temperature with Alexa 488-conjugated goat anti-mouse IgG (Molecular Probes) (1/400) in PBS. To see subcellular localization of the FLAG-tagged laTLRs, cells were treated with anti-FLAG Ab and Alexa 488 as described above and simultaneously stained with organella marker Abs; that is, rabbit anti-calnexin Ab (StressGen Biotechnologies) as an endoplasmic reticulum (ER) marker (1/200) or rabbit anti-EEA1 Ab (Affinity BioReagents) as an early endosome marker (4 μg/ml) and then Alexa 568-labeled goat anti-rabbit IgG for staining. The Golgi apparatus was stained with Texas Red-conjugated wheat germ agglutinin (1/100; Molecular Probes) and F-actin was stained by Phalloidin (1/500; Sigma-Aldrich. For acidic organelle staining, cells were pretreated with Lysotracker (final concentration of 1 mM) for 1 h before fixation. The stained cells were visualized at ×60 magnification under a FLUOVIEW microscope (Olympus). Images were captured using the attached computer software FLUOVIEW (26).

OL-17 cells were transfected with vectors and analyzed similarly to HeLa cells except for the transfection conditions, which are described in a previous report (23).

Immunohistochemical analysis

Formalin-fixed and paraffin-embedded sections were deparaffinized with xylene and rehydrated through a graded ethanol series. For Ag retrieval, sections were immersed in citrate buffer (pH 6.0) and heated using a pressure cooker. Thereafter, sections were treated with normal serum to eliminate nonspecific binding of Abs and incubated with 0.3% H_2O_2 methanol to quench endogenous peroxidase activity. After treatment, sections were incubated with rabbit anti-laTLR14b Ab (1/1000) at 4°C overnight. After incubation with EnVison goat anti-rabbit HRP-labeled second Ab (Dako-Cytomation), immunoreaction products were visualized with 3,3′-diaminobenzidine tetrahydrochloride (27, 28).

Results

cDNA cloning of lamprey TLRs

Many trials for the molecular cloning of lamprey TLRs were made with cDNAs prepared from an embryo of *L. japonica*. PCR amplification was successful using the primer set TLR16101 and TLR101R1 (Table I), which yielded a 210-bp cDNA fragment. A set of degenerate PCR primers was designed from conserved sequences (Fig. 1*A*; open rectangle) based on a homology search for TLR2 of various species (9, 29–31).

The cDNA fragment we cloned contained two distinct sequences encoding putative LRRs similar to those in huTLR2. By using the RACE method, the two sequences were extended over the pME18S-containing lamprey cDNA libraries (20). Finally, we identified two nucleotide sequences with putative open reading frames of LRRs and the TIR. We have prepared mRNAs from individual lampreys coming up the Ishikari river every year. The presence of this message was confirmed with adult lamprey gill mRNAs by sequencing 12 independent RT-PCR amplicons.

Deduced amino acid sequences from the cDNAs were analyzed by SMART programs, and the amino acid sequences are shown in Fig. 1*A*. Some LRR motifs and one TIR domain were predicted to exist. A hydrophobicity plot suggested that laTLR14a and 14b proteins are type I membrane proteins with signal peptides. These structures are shown in the Fig. 1*B*. These findings suggest that *L. japonica* has proteins of a TLR-like structure.

The two cloned laTLRs were highly homologous to each other (56% amino acid identities) (Fig. 1*C*). Recent BLASTP homology search analysis revealed that the laTLRs are most similar to the *T. rubripes* (pufferfish) TLR14 (fgTLR14) in the BLASTP database (Fig. 1*C* and Table II). We named these novel LRR-containing lamprey proteins laTLR14a and laTLR14b. The laTLR14a cDNA consisted of 2,486 bp, including an incomplete polyadenylation signal and poly(A) tail. This encoded a predicted protein of 815 amino acids whereas the laTLR14b cDNA consisted of 2,510 bp,

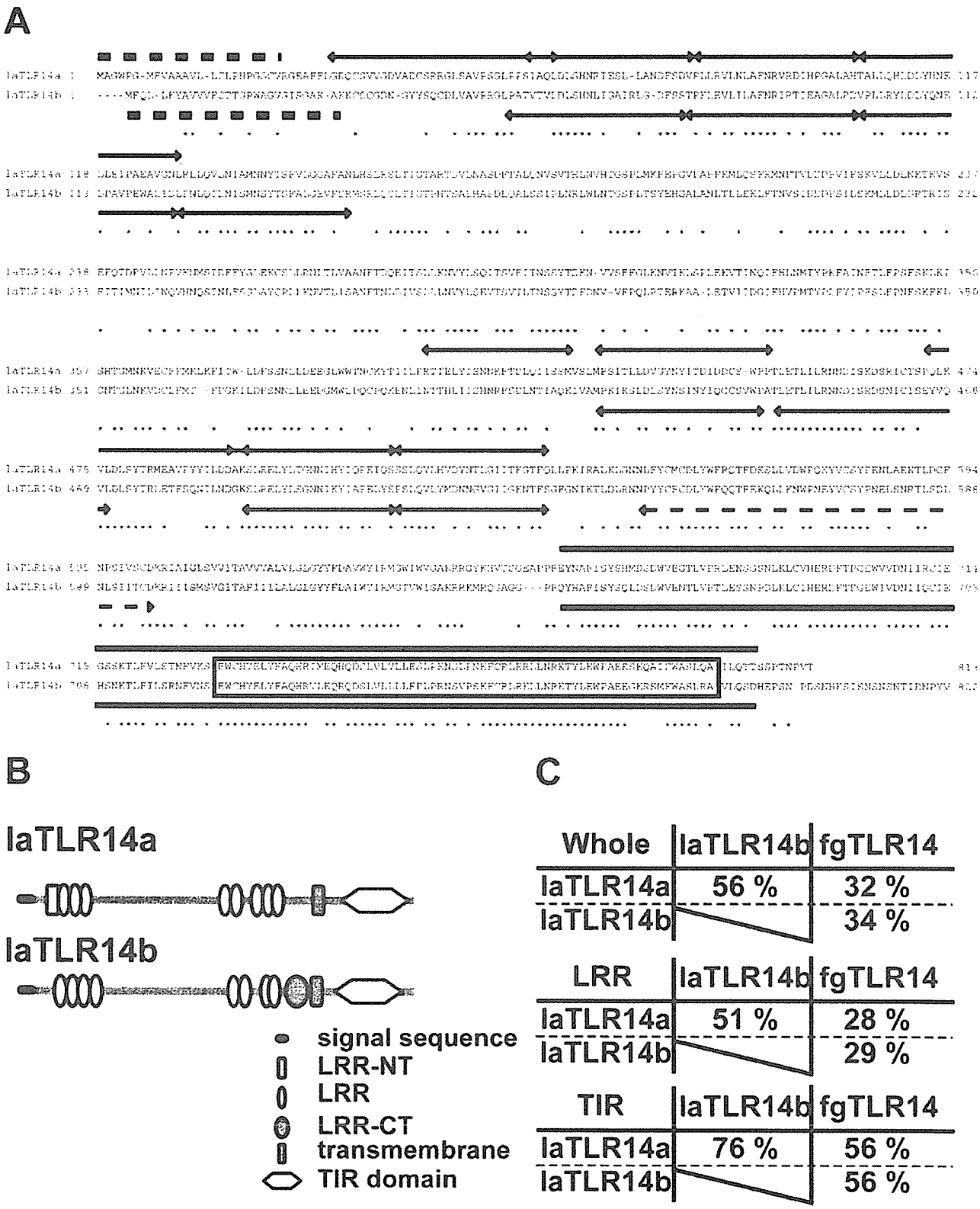

FIGURE 1. Amino acid alignment of cloned lamprey TLRs. *A*, Predicted amino acid sequences deduced from laTLR14a and laTLR14b cDNAs are aligned. Identical residues are indicated by asterisks, and each functional domain identified by the SMART program is shown by arrows (LRR-NT and LRR), gray box (TM), dotted arrow (C-terminal flanking region), dotted line (signal peptides), and solid line (TIR). *B*, Models of the predicted domain structures of laTLR14a and 14b. The LRR-CT domain of laTLR14a was not identified by SMART analysis. *C*, Percentage homology between fugu TLR14 (fgTLR14) and laTLR14a/b. The LRR and TIR regions are separately compared in the two *bottom tables*.

Table II. *Amino acid identities between fugu and lamprey TLRs*[a]

fgTLR	1	2	3	5	7	8	9	14	21	22	23
laTLR14a	30	29	21	23	Low	Low	Low	**33**	Low	23	Low
LRR[b]	25	26	21	23	Low	Low	Low	**27**	Low	24	Low
TIR[c]	47	44	30	31	36	38	35	**56**	42	40	39
laTLR14b	30	29	22	24	Low	Low	Low	**34**	Low	24	Low
LRR	26	24	21	23	Low	Low	Low	**29**	Low	24	Low
TIR	50	46	27	29	36	39	34	**58**	42	42	40

[a] The values of identities are indicated as a percentage, and the highest values are shown by bold numbers. Low, Percentage of similarity is too low to determine.
[b] LRR domain of laTLR14.
[c] TIR domain of laTLR14.

encoding a predicted protein of 822 amino acids (Fig. 1*A*). laTLR14a consisted of one unique N-terminal LRR-like motif (named LRR-NT), seven typical LRR motifs, one unique C-terminal LRR motif (named LRR-CT), followed by a transmembrane domain and a TIR domain (Fig. 1*C*). TLR14b structurally resembled TLR14a except for the lack of LRR-NT sequence. The TIRs of laTLR14a/b are most similar to that of fgTLR14 (>50% of amino acid identities). However, laTLR14a and laTLR14b exhibited only 29–34% identity to fgTLR14 in overall similarity (data not shown). The LRR domains of laTLR14 were <30% homologous to those of the huTLR2 subfamily, huTLR1, 2 6, and 10, although their TIR domains were >50% homologous (Table II). Bootstrap probability analysis suggested that TLR14 evolved from M-type TLR2 (Fig. 2 and Ref. 17). It is possible that laTLR14s were derived from the ancestral M-type TLR2 before the lamprey separated from fish and that laTLR14a and 14b diverged more recently after the lamprey species diverged from fish (Fig. 2). Hence, we suggest that the agnathan lamprey has structural orthologs of the gnathostome TLR system.

Protein expression of laTLRs

Protein expression and subcellular localization of laTLRs were analyzed in human HEK293 cells. We used pEFBOS-FLAG vector, which has the elongation factor promoter. Proteins of laTLR14a and laTLR14b with FLAG (either C-terminal or N-terminal) were detected by immunoblotting, flow cytometry, and immunofluorescence staining. laTLR14b (C-terminal FLAG) gave a thick protein band of 85 kDa and a thin band of 105 kDa by immunoblotting using an anti-FLAG Ab (Fig. 3*A*). This two-band profile was reproducible on the blot by using an Ab against laTLR14b (Fig. 3*A*). Only the 85-kDa band was detected in the lane with laTLR14a (C-terminal) in the blot using anti-FLAG Ab (Fig. 3*A*). The laTLR14b protein could be detected with the anti-laTLR14b Ab as well as anti-FLAG Ab (Fig. 3*A*). The molecular mass of 85 kDa is consistent with those expected from the two cDNA sequences of laTLRs. The 105-kDa protein form may be generated through posttranslational modifications.

By using flow cytometry with an anti-FLAG Ab, HEK293 cells expressing N-terminal laTLR14a or 14b were analyzed. laTLR14a (data not shown) and laTLR14b (Fig. 3*B*) were not detected on the surface of the transfected HEK cells. The laTLR14b with C-terminal FLAG showed a similar result (data not shown). When the cells were permeabilized and probed with anti-FLAG Ab (Fig. 3*C*), laTLR14b (C-terminal FLAG) was detected in the M1-positive gate by flow cytometry. Ultimately, ~10% of the transfected HEK cells expressed laTLR14b inside the cells.

We next probed laTLR14b in lamprey cells with the Ab against laTLR14b. The lamprey gill specimen was immunohistochemically stained using the Ab against laTLR14b. Some of cells in the epithelium of the lamprey gill were laTLR14b-positive (Fig. 3*D*), although the signal of laTLR14b was not very strong. laTLR14b appeared to reside inside the cells, consistent with the results of ectopic expression studies on laTLR14.

To see the localization of laTLRs in organelles, cells overexpressing laTLR14a and 14b were analyzed by a confocal microscope (Fig. 4). Two cell lines of human and fish were used for laTLR14 localization analysis. In human HeLa cells, FLAG-tagged laTLR14a and 14b were merged with the ER marker calnexin (Fig. 4A, *upper rows*), but not with markers for the Golgi apparatus (Fig. 4*A*, *lower rows*), endosomes, lysosomes, and F-actin (data not shown). In medaka OL-17 cells, the majority of the laTLR14 populations were localized to the ER, although some of them were distributed in other organelles (Fig. 4B, *upper rows*) but not merged with the Golgi apparatus (Fig. 4*B*, *lower rows*). Thus, like TLR9 as reported previously (32), laTLR14a and 14b are largely localized to the ER and only partly moved to other organelles.

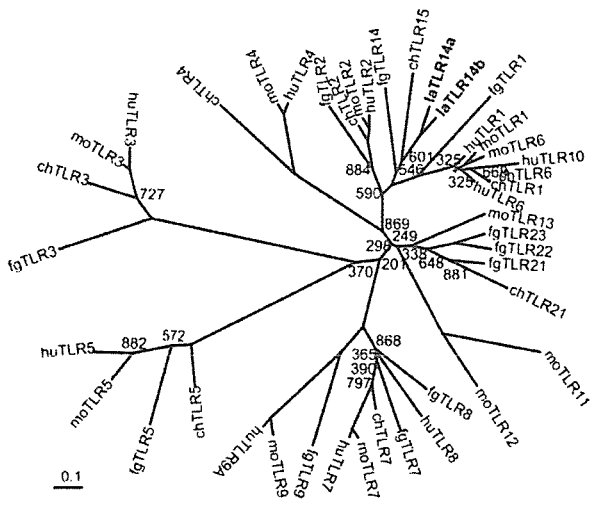

FIGURE 2. Phylogenetic tree for laTLR14a/b. Phylogenetic tree of puffer fish (fg), chicken (ch), mouse (mo), human (hu), and lamprey (la) TLRs. The amino acid sequences of the TIR domains were subjected to analysis. Bootstrap values (<900) are shown. Lamprey TLRs belonging to the TLR2 family are shown by bold characters.

Reporter assay for determination of promoter activation by laTLRs

Various ligands for huTLRs were tested to see whether they activate laTLR14a or 14b. The human HEK293 system with reporter genes was used because it can detect signals of fish and lamprey TLRs (33) (A. Ishii and T. Seya, unpublished data). Macrophage-activating lipopeptide-2, Pam3, *S. aureus* peptidoglycan, poly(I:C), LPS, and flagellin failed to elicit laTLR14a/b activation in

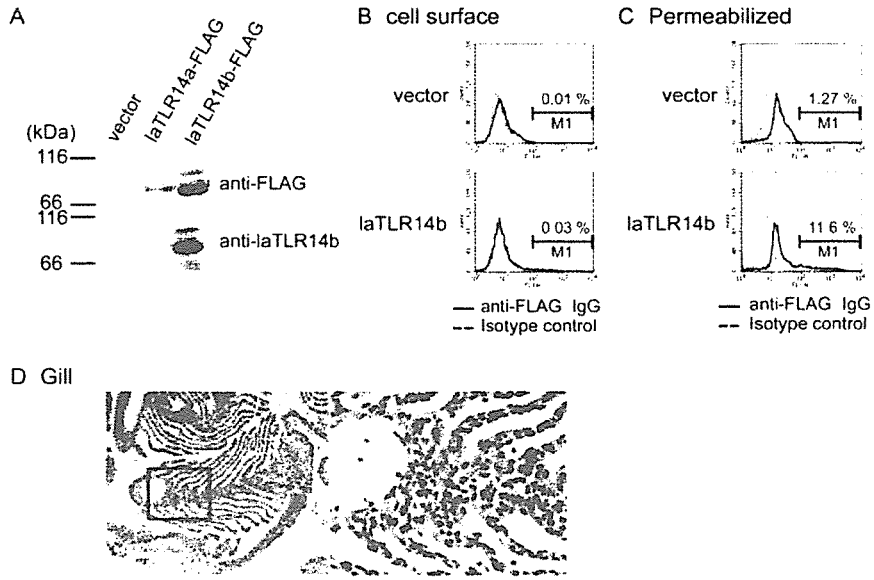

FIGURE 3. Protein expression analysis of laTLR14a/b. *A*, Immunoblotting. Plasmids containing C-terminal FLAG-tagged cDNAs of laTLR14a and laTLR14b were transfected into HEK293 cells. After 24 h, cells were solubilized and lysates were collected for immunoblotting. The blots were probed with an anti-FLAG Ab or an anti-laTLR14b Ab. The control contained only the vector. Molecular mass values are shown to the *left*. The minor bands above the laTLR14b protein may be a secondary product generated through modification. *B* and *C*, Flow cytometric analysis for surface-expressed and intracellular TLRs. HEK293 cells were transfected with vectors that allow the expression of an N-terminal FLAG-tagged laTLR14b protein. After 24 h, cells were treated first with anti-FLAG Ab and then with FITC-labeled goat anti-rabbit IgG Ab. Isotype-matched IgG was used as a control for the first Ab. laTLR14a was barely detectable with anti-FLAG Ab (data not shown). Intracellular TLRs were detected in permeabilized cells. Similar results were obtained using C-terminal-tagged constructs (data not shown). Percentages of cells in the M region are indicated. Three independent experiments gave similar results. A representative profile using the N-terminal tagged construct is given. *D*, Immunohistochemical staining of lamprey gills by an Ab against laTLR14b. The specimens were stained with an anti-laTLR14b Ab and a HRP-labeled second Ab. Nonimmune rabbit IgG was used as a negative control (not shown). *Left panel*, Original magnification, ×80; *right panel*, the marked region is enlarged (original magnification, ×400).

terms of NF-κB and the IFN-β promoter at the doses at which they activate huTLRs (data not shown). The reporters did not specifically respond to these reagents even with different transfection methods (data not shown). No significant increase of reporter was observed with any bacterial extract tested (*C. sporogenes and S. typhimurium*) for activation of laTLR14a/b (data not shown).

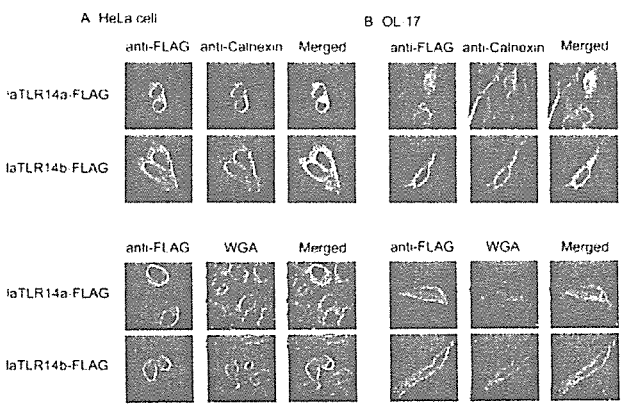

FIGURE 4. Subcellular localization of laTLR14a/b. HeLa cells (*A*) or medaka (Hd-rR) OL-17 cells (*B*) attached to coverslips were transfected with plasmid of laTLR14a or 14b (C-terminal FLAG-tagged). Twenty-four hours after transfection, cells were incubated with organelle markers for 1 h. FLAG-tagged proteins were stained with anti-FLAG Ab and imaged by confocal microscopy. The yellow staining in the overlay indicates co-localization of laTLR14. Examples for the colocalization analysis are shown for ER (calnexin) (*upper panels*) and Golgi (wheat-germ agglutinin (WGA)) (*bottom panels*). A predominant ER merging profile was observed in human HeLa cells as well as OL-17 fish cells (*B*), which were pretreated similarly to HeLa cells. Results of one of the three representative experiments is shown.

Functional analysis of the CD4-laTLR14b chimera protein

We next investigated whether the reporter is activated by the chimera construction with extracellular CD4 and intracellular laTLR14a or 14b by using HEK293 human reporter analysis. The Ig-like domains of human CD4 were ligated with the transmembrane and intracellular regions of laTLR14a or 14b (Fig. 5*A*). Flow cytometric analysis showed that ~3.6% of CD4-laTLR14a and 15% of CD4-laTLR14b were expressed on the surface of the transfected HEK293 cells (M1 region in Fig. 5*B*). Using the ELAM promoter and the p-125 luc promoter, we examined whether the chimera laTLR14a or laTLR14b elicits activation of the NF-κB and IFN-β promoter by CD4 dimerization. CD4-laTLR14b induced ELAM promoter-mediated NF-κB activation (Fig. 5*C*). The activation of NF-κB was suppressed by cotransfection of the MyD88 dominant negative form, suggesting that laTLR14b activates NF-κB via human MyD88. Human Mal and the Toll-IL-1R domain-containing adaptor molecule (TICAM)-1 appear not to be involved in the TLR14-mediated NF-κB activation pathway (Fig. 5*C*). CD4-laTLR14b only marginally induced IFN-β promoter activation, which was completely inhibited by cotransfection with MyD88 dominant negative in HEK cells (data not shown). The minute IFN-β promoter activation appears to be induced secondarily via MyD88 and NF-κB. Thus, laTLR14b is a signaling receptor for the activation of NF-κB in the human cell system.

Even though CD4-laTLR14a was slightly expressed on the surface of HEK transfectants, it barely induced signaling in response to CD4 dimerization (data not shown).

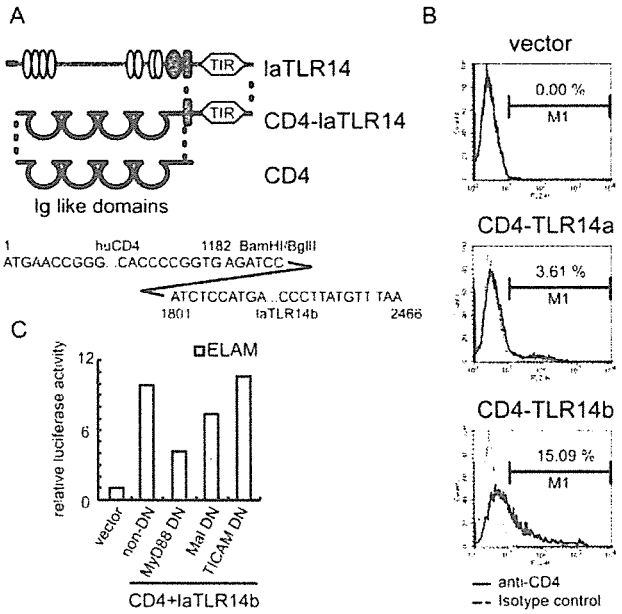

FIGURE 5. laTLR14b activates NF-κB via MyD88 in human cells. *A*, Constructions of constitutive active forms of laTLR14a (CD4-TLR14a) and laTLR14b (CD4-TLR14b). The sequence of fused cDNAs extracellular domains of human CD4 and each TIR domain of laTLRs is shown. *B*, Expression of the fused proteins in HEK293 cells. Twenty-four hours after transfection of the indicated cDNAs into HEK293 cells, the protein expression levels of CD4-TLR14a and 14b on the cell surface were measured by flow cytometry using anti-CD4 Ab conjugated with PE. Protein expression is barely detectable in cells transfected with the empty vector (*top*) or CD4-TLR14a cDNA (*center*). Only CD4-TLR14b expression is detectable on the surface (*bottom*). *C*, Luciferase reporter assay was performed to measure the levels of activation of NF-κB. An empty vector and each CD4-TLR14 construct were transfected into HEK293 cells together with an ELAM-luciferase reporter plasmid. The dominant negative (DN) forms of MyD88 (MyD88 DN), Mal/TIRAP (Mal DN), or TICAM-1 (TICAM DN) were simultaneously expressed in HEK293 cells in addition to the above proteins as described in the *Materials and Methods*. After 24 h, luciferase activities in cell lysates were measured. Relative luciferase activities are shown as described previously for determination of activation of NF-κB (26). Experiments were performed in triplicate. Results of one of the three experiments is shown.

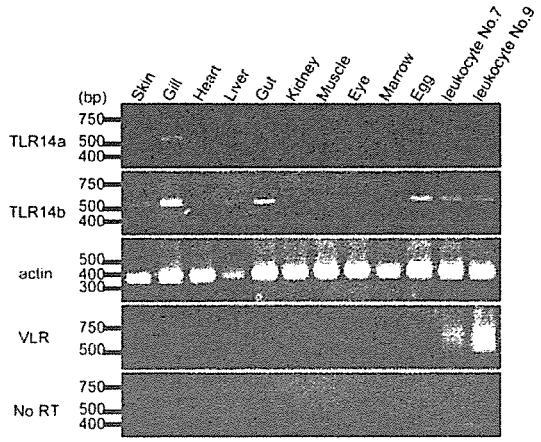

FIGURE 6. Tissue distribution of laTLR14a/b in comparison with VLR. Tissue distribution of mRNA of laTLRs in *L. japonica* organs. Amplifications of TLR gene fragments were accomplished by the RT-PCR technique using equal numbers of PCR cycles. Cytoskeletal actin (actin) of lamprey was used for a positive control, and templates without reverse transcriptase (no RT) were used for a negative control. The control PCRs were performed with all of the primer sets indicated in the figure and no band was detected (data not shown). Results using the actin primers are shown here. cDNAs were prepared from total RNA in each tissue from 13 individual lampreys. The conditions of the PCR analysis are described in the *Materials and Methods*. Amplified DNA fragments were electrophoresed in 1% agarose gel and visualized by ethidium bromide staining. A representative mRNA distribution profile obtained by PCR analysis is shown here because similar results were obtained with each individual regarding the laTLR14a/b distribution profiles. VLR is exclusively expressed in lamprey leukocytes, but the VLR mRNA levels appear to be different among individuals. Examples are shown with leukocytes (animals no. 7 and no. 9).

Comparison of laTLRs with VLR

Distribution of laTLR14a and 14b were determined by RT-RCR using cDNAs from various tissues as templates. For this purpose, lampreys were harvested in the Ishikari river every winter for 5 years. Individual lamprey showed similar laTLR14a/b mRNA expression profiles (Fig. 6). laTLR14a mRNA was exclusively expressed in the gills of lampreys. In contrast, laTLR14b mRNA was expressed in the skin, gills, heart, liver, gut, and leukocytes (Fig. 6). The strongest signal was obtained in the gill and gut. We could not confirm the results by immunoblotting or histochemical staining using the anti-laTLR14b Ab (data not shown), which may reflect the low protein expression levels of this protein in various organs.

It has been reported that lampreys express proteins with various sets of tandemly arranged LRRs named VLRs in their lymphocyte-like cells and that VLRs are related to the lamprey immune system (12, 13). We isolated these cells as described earlier (11), extracted RNA, and confirmed the existence of VLR messages using RT-PCR (Fig. 6). The VLR mRNAs were unequivocally detected in leukocytes but too faint to see in other organs by ethidium bromide staining. The VLR mRNA bands were detectable in the organs including the gill, heart, and gut after repetitive PCR (data not shown). It is likely that the origin of the VLR mRNAs is blood leukocytes. The results showed that leukocytes express both laTLR14b and VLR. Based on the broad PCR bands corresponding to VLR, its primary sequences appeared to be variable. To determine actual nucleotide sequences of the VLRs, we cloned the PCR amplicons and sequenced. The alignment of the representative amino acid sequences is shown in Fig. 7*A*. In contrast, laTLR14b from the same individual did not show such high rates of variation or heterogeneity in their sequences (Fig. 7*B*). The sequence invariability of laTLR14b was confirmed with four individual lampreys harvested in different years (data not shown). The single amino acid substitutions were observed in the sequences of laTLR14b, probably due to artifacts of polymerase misreading. Hence, the heterogeneity occurs selectively in VLRs but not in TLRs in lampreys. The lamprey TLRs, at least TLR14a and 14b, evolved independently of the VLR family, resulting in the formation of a distinct LRR system with differential functions.

Discussion

In this study, we demonstrated the following. First, the lamprey possesses type I membrane proteins consisting of LRRs and the TIR domain that may be classified into the TLR family based on their structure. We call these proteins laTLR14a and laTLR14b. Second, the localization analysis in human and fish cell lines revealed that the lamprey TLR-like proteins largely reside in the cytoplasmic compartment ER in human cells. In transfected fish cell lines, the laTLR14s were localized to the ER and other organelles.

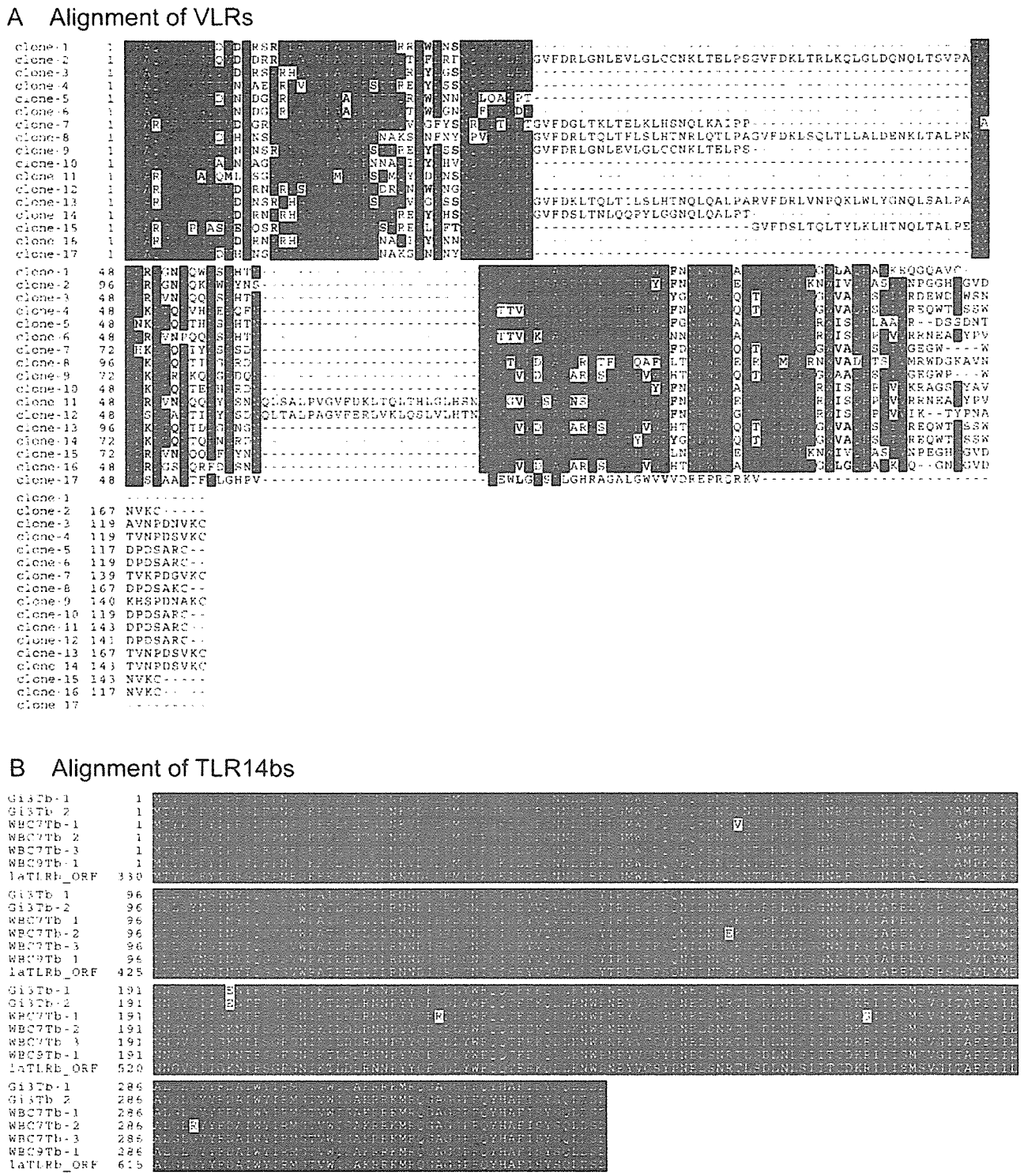

FIGURE 7. VLRs in the lamprey. *A*, Alignment of amino acid sequences of part of LRRs in VLR and TLR in the lamprey. Seventeen *L. japonica* VLRs were cloned from the mRNA of gill (animals no. 1 to no. 5), gut (animals no. 6 to no. 10) and leukocytes (animals no. 11 to no. 17). The VLR clones may be originated from blood leukocytes. laTLR14b DNA fragments were cloned from cDNA libraries of three individual fish (animals no. 3, no. 7, and no. 9) *B*, Gi, gill; WBC, white blood cells. The cloned laTLR14b fragments did not exhibit any diversity like VLRs. The identical residues are shaded by BOXSHADE program (www.ch.embnet.org/software/BOX_form.html).

Third, NF-κB and IFN-β promoter activation was promoted in human cells by artificial dimerization of the lamprey protein laTLR14b. Fourth, Lamprey TLR proteins existed structurally independent of VLR; these TLR proteins were neither variable in their primary sequences nor expected to have GPI anchors. Fifth, laTLR14b was preferentially expressed in the gills, gut, and leukocytes. Thus, the lamprey most likely has immune-related TLRs structurally distinguished from the reported VLR proteins. In TLRs, the LRR motif serves to

recognize microbial patterns and signatures and the TIR participates in intracellular signaling. The functional results for laTLR14b overexpressed in human cells are at least compatible with those for TLRs of other species. Yet, the pattern for recognition by this laTLR remains unknown. Further investigation is needed to determine whether the lamprey TLRs are localized to putative macrophages/monocytes. These cells may differ from lamprey lymphocytes, which have been shown to be VLR-positive cells.

Our data also suggest that the lamprey protein laTLR14b is capable of activating the huTLR signal pathways. In fish and chicken TLRs, their functions can be determined by a reporter assay with human cells expressing a CD4-TIR chimera or dominant negative proteins. That is, the chicken TLR2 signals the presence of lipoproteins even in the human system (34). The fish TLR5 and TLR21 recognize flagellin and poly(I:C) (19) (A. Matsuo and T. Seya, unpublished data), respectively, to induce activation of the NF-κB and IFN-β promoter in human cells (33, 34). Thus, we currently hold that human MyD88 is associated with laTLR14b-mediated NF-κB and secondary IFN-β promoter activation according to the results of chimera and dominant negative experiments. The results show the likelihood that lamprey TLRs act as pattern recognition receptors and transmit signals to downstream adapter proteins in host cells. For final confirmation, however, we must examine the protein function in a system using lamprey cell lines (which are not yet available).

The two lamprey TLRs belong to the subfamily of TLR14. laTLR14a/b most resemble each other and their TIRs are ~50% homologous to that of huTLR2. Gene duplication of TLR14 ortholog may have resulted in the two TLR14 genes in the lamprey. TLR14 and TLR2 do not appear to be duplicated in fish. However, a TLR2 pseudogene appears upstream in tandem with the functional TLR2 in the opossum, dog, and human (6). The pseudogene is probably from a duplication event before the divergence of marsupials. Likewise, a putative duplication event may have caused the two lamprey TLRs.

T. rubripes has a set of TLRs similar to those of the human and mouse (9) and orthologs of MyD88, Mal/TIRAP, and TICAM (a single gene representative of TICAM-1 and TICAM-2) (A. Matsu and T. Seya, unpublished data). The fish TLR system is structurally and functionally comparable with those of the human and mouse. Only minor functional variations appear to have occurred during evolution of the vertebrate TLR system, and the fundamental functional properties of the TLR system are conserved across fish and humans. Our present results may present a key to prove that the lamprey possesses orthologs of the mammalian TLR system and adapters.

L. japonica cells discard part of their genome during maturation (18). Their genome properties may be changed year to year. We have surveyed the mRNAs of laTLR14b and VLR for 5 years. Leukocytes of all individual lampreys expressed laTLR14 (a/b) and VLRs for all 5 years. Distributions of laTLR14b in lampreys were similar among individual fish. More limited expression of TLR14a than TLR14b was observed in all individuals tested. Thus, the laTLR14b protein, which is the ortholog of immune-related TLR, is actually expressed in the gills of live lampreys.

TLR1, 2, 6, and 10 are members of the TLR2 subfamily. In humans and mice, TLR2 recognizes diacylated mycoplasma lipoproteins in combination with TLR6 and triacylated bacterial lipoproteins together with TLR1 (25, 35, 36). If TLR14 is a member of the TLR2 subfamily, laTLR14 might recognize some microbial patterns in concert with another TLR2 member protein. Thus, we investigated whether lamprey and fish TLR14 exerts its function with huTLR2 members. However, laTLR14a/b, as well as fish TLR14, did not activate NF-κB even by coexpression with huTLR2 or other TLR2 members under the condition of stimulation with bacterial lipoproteins or other known TLR ligands (data not shown). Only a chimera version consisting of extracellular CD4 and the TIR domain of laTLR14b activates NF-κB as previously reported for huTLR4 and mouse TLR6, which activate NF-κB via their CD4-mediated dimerization (1, 22). Because TLR14 is found in *T. rubripes* (fgTLR14) (6), *D. rerio*, and *X. tropicalis* but not in human, mouse and chicken, its ligand may be a component of microorganisms in water.

The genomes of *Drosophila* and the mosquito *A. gambiae* contain ~10 Toll homologues, but only a few participate in host immunity (7, 8). Others are linked to developmental functions. Likewise, immune function could not be attributed to the single Toll homologue of *Caenorhabditis elegans* (37) and *Caenorhabditis briggsae* or to the TLRs reported in the horseshoe crab *Tachypleus tridentatus* (1). In contrast, the genome of the sea urchin *Strongylocentrotus purpuratus* abounds with TLR-containing genes, presumably >300 (6, 7). The genomes of the amphioxus *Brachiostoma floridae* and the solitary tunicate *Ciona savignyi* contain >10 TLR genes (7). The protostome and deuterostome invertebrates appear to have been differentially evolved in terms of the TLR system. The differences in the TLR system may reflect the differences in the microbial environment where each species of invertebrates survives. A critical factor for the selection of the TLR system would be infection.

It has been reported that the lamprey responds to some extent to some adjuvants (38) that we have revealed as TLR agonists. In addition, the lamprey possesses a complement-like molecule that opsonizes rabbit erythrocytes (39). Later, the lamprey had been shown to have the complement system including C3 and its activation and inactivation cascades (20, 40). Major family for complement regulatory proteins consists of short consensus repeats, and the lamprey possesses a short consensus repeat-containing complement-inhibitory protein named lacrep (20). The lamprey also expresses many C-type lectins like those in *Ciona intestinalis* (41, 42). However, whether or not the TLR pathogen-recognition system is conserved in jawless fish has remained unclear at a molecular level. Our results regarding two lamprey TLRs of the TLR2 subfamily add some pieces of knowledge to the vertebrate innate immune system. The lamprey possesses a pattern recognition system involving the complement and its regulatory systems, C-type lectins, and the TLR system as observed in higher vertebrates, including humans.

Acknowledgments

We are grateful to Dr. K. Funami, Dr. M. Shingai, M. Sasai, and K. Higuchi in our laboratory for critical discussions. Thanks are also due to Dr. H. Mitani (Tokyo University, Tokyo, Japan) for providing OL-17 cells. Dr. V. Kumar (St. Louis University, St. Louis, MO) reviewed this manuscript before submission.

Disclosures

The authors have no financial conflict of interest.

References

1. Medzhitov, R., P. Preston-Hurlburt, and C. A. Janeway. 1997. A human homologue of the *Drosophila* Toll protein signals activation of adaptive immunity. *Nature* 388: 394–397.
2. Xu, Y., X. Tao, B. Shen, T. Horng, R. Medzhitov, J. L. Manley, and L. Tong. 2000. Structural basis for signal transduction by the Toll/interleukin-1 receptor domains. *Nature* 408: 111–115.
3. Bell, J. K., I. Botos, P. R. Hall, J. Askins, J. Shiloach, D. M. Segal, and D. R. Davies. 2005. The molecular structure of the Toll-like receptor 3 ligand-binding domain. *Proc. Natl. Acad. Sci. USA* 102: 10976–11080.
4. Choe, J., M. S. Kelker, and I. A. Wilson. 2005. Crystal structure of human toll-like receptor 3 (TLR3) ectodomain. *Science* 309: 581–585.

5. Lemaitre, B., E. Nicolas, L. Michaut, J. M. Reichhart, and J. A. Hoffmann. 1996. The dorsoventral regulatory gene cassette spatzle/Toll/cactus controls the potent antifungal response in *Drosophila* adults. *Cell* 86: 973–983.
6. Roach, J. C., G. Glusman, L. Rowen, A. Kaur, M. K. Purcell, K. D. Smith, L. E. Hood, and A. Aderem. 2005. The evolution of vertebrate Toll-like receptors. *Proc. Natl. Acad. Sci. USA* 102: 9577–9582.
7. Pancer, Z., and M. D. Cooper. 2006. The evolution of adaptive immunity. *Ann. Rev. Immunol.* 24: 497–518.
8. Imler, J. L., and J. A. Hoffmann. 2002. Toll receptors in *Drosophila*: a family of molecules regulating development and immunity. *Curr. Top. Microbiol. Immunol.* 270: 63–79.
9. Oshiumi, H., T. Tsujita, K. Shida, M. Matsumoto, K. Ikeo, and T. Seya. 2003. Prediction of the prototype of the human Toll-like receptor gene family from the pufferfish *Fugu rubripes* genome. *Immunogenetics* 54: 791–800.
10. Medzhitov, R. 2001. Toll-like receptors and innate immunity. *Nat. Rev. Immunol.* 1: 135–145.
11. Uinuk-Ool, T., W. E. Mayer, A. Sato, R. Dongak, M. D. Cooper, and J. Klein. 2002. Lamprey lymphocyte-like cells express homologs of genes involved in immunologically relevant activities of mammalian lymphocytes. *Proc. Natl. Acad. Sci. USA* 99: 14356–14361.
12. Pancer, Z., C. T. Amemiya, G. R. Ehrhardt, J. Ceitlin, G. L. Gartland, and M. D. Cooper. 2004. Somatic diversification of variable lymphocyte receptors in the agnathan sea lamprey. *Nature* 430: 174–180.
13. Alder, M. N., I. B. Rogozin, L. M. Iyer, G. V. Glazko, M. D. Cooper, and Z. Pancer. 2005. Diversity and function of adaptive immune receptors in a jawless vertebrate. *Science* 310: 1970–1973.
14. Pancer, Z., N. R. Saha, J. Kasamatsu, T. Suzuki, C. T. Amemiya, M. Kasahara, and M. D. Cooper. 2005. Variable lymphocyte receptors in hagfish. *Proc. Natl. Acad. Sci. USA* 102: 9224–9249.
15. Takeda, K., T. Kaisho, and S. Akira. 2003. Toll-like receptors. *Annu. Rev. Immunol.* 21: 335–376.
16. Iwasaki, A., and R. Medzhitov. 2004. Toll-like receptor control of the adaptive immune responses. *Nat. Immunol.* 10: 987–995.
17. Overath, P., J. Ruoff, Y. D. Stierhof, J. Haag, H. Tichy, I. Dykova, and J. Lom. 1998. Cultivation of bloodstream forms of *Trypanosoma carassii*, a common parasite of freshwater fish. *Parasitol. Res.* 84: 343–347.
18. Kohno, S., Y. Nakai, S. Satoh, M. Yoshida, and H. Kobayashi. 1986. Chromosome elimination in the Japanese hagfish. *Eptatretus burgeri* (Agnatha, Cyclostomata). *Cytogenet. Cell Genet.* 41: 209–214.
19. Tsujita, T., A. Ishii, H. Tsukada, M. Matsumoto, F.-S. Che, and T. Seya. 2006. Fish soluble Toll-like receptor (TLR)5 amplifies human TLR5 response via physical binding to flagellin. *Vaccine* 24: 2193–2199.
20. Kimura, Y., N. Inoue, A. Fukui, H. Oshiumi, M. Matsumoto, M. Nonaka, S. Kuratani, T. Fujita, M. Nonaka, and T. Seya. 2004. A short consensus repeat-containing complement regulatory protein of lamprey that participates in cleavage of lamprey complement 3. *J. Immunol.* 173: 1118–1128.
21. Matsumoto, M., S. Kikkawa, M. Kohase, K. Miyake, and T. Seya. 2002. Establishment of a monoclonal antibody against human Toll-like receptor 3 that blocks double-stranded RNA-mediated signaling. *Biochem. Biophys. Res. Commun.* 293: 1364–1369.
22. Takeuchi, O., T. Kawai, H. Sanjo, N. G. Copeland, D. J. Gilbert, N. A. Jenkins, K. Takeda, and A. Akira. 1999. TLR6: A novel member of an expanding toll-like receptor family. *Gene* 231: 59–65.
23. Komura, J., H. Mitani, and A. Shima. 1988. Fish cell culture: establishment of two fibroblast-like cell lines (OL-17 and OL-32) from fins of the medaka *Oryzias latipes*. *In Vitro Cell. Dev. Biol.* 24: 294–298.
24. Inoue, N., A. Fukui, M. Nomura, M. Matsumoto, K. Toyoshima, and T. Seya. 2001. A novel chicken membrane-associated complement-regulatory protein: molecular cloning and functional characterization of a chicken membrane SCR protein. *J. Immunol.* 166: 424–431.
25. Nishiguchi, M., M. Matsumoto, T. Takao, M. Hoshino, Y. Shimonishi, S. Tsuji, O. Takeuchi, S. Akira, K. Toyoshima, and T. Seya. 2001. *Mycoplasma fermentans* lipoprotein M161Ag-induced cell activation is mediated by Toll-like receptor 2: Role of N-terminal hydrophobic portion in its multiple functions. *J. Immunol.* 166: 2610–2616.
26. Nakao, Y., K. Funami, S. Kikkawa, M. Taniguchi, M. Nishiguchi, Y. Fukumori, T. Seya, and M. Matsumoto. 2005. Surface-expressed TLR 6 participates in the recognition of diacylated lipopeptide and peptidoglycan in human cells. *J. Immunol.* 174: 1566–1573.
27. Okada, Y., H. Sawa, S. Endo, Y. Orba, T. Umemura, H. Nishihara, A. C. Stan, S. Tanaka, and K. Nagashima. 2002. Expression of JC virus (JCV) agnoprotein in progressive multifocal leukoencephalopathy (PML) brain. *Acta Neuropathol.* 104: 130–136.
28. Sunden, Y., T. Suzuki, Y. Orba, T. Umemura, M. Asamoto, K. Nagashima, S. Tanaka, and H. Sawa. 2006 Characterization and application of polyclonal antibodies that specifically recognize JC virus large T antigen. *Acta Neuropathol.* 111: 379–387.
29. Jault, C., L. Pichon, and J. Chluba. 2004. Toll-like receptor gene family and TIR-domain adapters in *Danio rerio*. *Mol. Immunol.* 40: 759–771.
30. Meijer, A. H., S. F. Gabby Krens, I. A. Medina Rodriguez, S. He, W. Bitter, B. Ewa Snaar-Jagalska, and H. P. Spaink. 2004. Expression analysis of the Toll-like receptor and TIR domain adaptor families of zebrafish. *Mol. Immunol.* 40: 773–783.
31. Yilmaz, A., S. Shen, D. L. Adelson, S. Xavier, and J. J. Zhu. 2005. Identification and sequence analysis of chicken Toll-like receptors. *Immunogenetics* 56: 743–753.
32. Latz, E., A. Schoenemeyer, A. Visintin, K. A. Fitzgerald, B. G. Monks, C. F. Knetter, E. Lien, N. J. Nilsen, T. Espevik, and D. T. Golenbock. 2004. TLR9 signals after translocating from the ER to CpG DNA in the lysosome. *Nat. Immunol.* 5: 190–198.
33. Tsujita, T., H. Tsukada, M. Nakao, H. Oshiumi, M. Matsumoto, and T. Seya. 2004. Sensing bacterial flagellin by membrane and soluble orthologs of Toll-like receptor 5 in rainbow trout (*Onchorhynchus mikiss*). *J. Biol. Chem.* 279: 487588–48597.
34. Fukui, A., N, Inoue, M. Matsumoto, M. Nomura, Y., Matsuda, K. Toyoshima, and T. Seya. 2001. Molecular cloning and functional characterization of chicken Toll-like receptors. *J. Biol. Chem.* 276: 47143–47149.
35. Takeda, K., O. Takeuchi, and S. Akira. 2002. Recognition of lipopeptides by Toll-like receptors. *J. Endotoxin Res.* 8: 459–463.
36. Ozinsky, A., D. M. Underhill, J. D. Fontenot, A. M. Hajjar, K. D. Smith, C. B. Wilson, L. Schroeder, and A. Aderem. 2000. The repertoire for pattern recognition of pathogens by the innate immune system is defined by cooperation between Toll-like receptors. *Proc. Natl. Acad. Sci. USA* 97: 13766–13771.
37. Couillault, C., N. Pujol, J. Reboul, L. Sabatier, J. F. Guichou, Y. Kohara, and J. J. Ewbank. 2004. TLR-independent control of innate immunity in *Caenorhabditis elegans* by the TIR domain adaptor protein TIR-1, an ortholog of human SARM. *Nat. Immunol.* 5: 488–494.
38. Finstad, J., and R. A. Good. 1964. The evolution of the immune response. III. Immunologic responses in the lamprey. *J. Exp. Med.* 120: 1151–1168.
39. Nonaka, M., T. Fujii, T. Kaidoh, S. Natsuume-Sakai, M. Nonaka, N. Yamaguchi, and M. Takahashi. 1984. Purification of a lamprey complement protein homologous to the third component of the mammalian complement system. *J. Immunol.* 133: 3242–3249.
40. Nonaka, M., and M. Takahashi. 1992. Complete complementary DNA sequence of the third component of complement of lamprey. Implication for the evolution of thioester containing proteins. *J. Immunol.* 148: 3290–3295.
41. Schluter, S. F., J. Schroeder, E. Wang, and J. J. Marchalonis. 1994. Recognition molecules and immunoglobulin domains in invertebrates. *Ann. NY Acad. Sci.* 712: 74–81.
42. Azumi, K., R. De Santis, A. De Tomaso, I. Rigoutsos, F. Yoshizaki, M. R. Pinto, R. Marino, K. Shida, M. Ikeda, M. Ikeda, et al. 2003. Genomic analysis of immunity in a Urochordate and the emergence of the vertebrate immune system. *Immunogenetics* 55: 570–581.

NAK-Associated Protein 1 Participates in Both the TLR3 and the Cytoplasmic Pathways in Type I IFN Induction[1]

Miwa Sasai,*† Masashi Shingai,* Kenji Funami,* Mitsutoshi Yoneyama,‡ Takashi Fujita,‡ Misako Matsumoto,*†§ and Tsukasa Seya[2]*§

TLR3 and the cytoplasmic helicase family proteins (retinoic acid-inducible gene I (RIG-I) and melanoma differentiation-associated gene 5 (MDA5)) serve as dsRNA pattern-recognition receptors. In response to poly(I:C), a representative of dsRNA, and viral infection, they have been shown to activate the transcription factor IFN regulatory factor (IRF)-3, which in turn induces activation of the IFN-β promoter. RIG-I/MDA5 recognizes dsRNA in the cytoplasm, whereas TLR3 resides in the cell surface membrane or endosomes to engage in extracytoplasmic recognition of dsRNA. Recent reports suggest that TLR3 induces cellular responses in epithelial cells in response to respiratory syncytial virus (RSV). The modus for TLR3 activation by RSV, however, remains unresolved. By small interference RNA gene-silencing technology and human cell transfectants, we have revealed that knockdown of NAK-associated protein 1 (NAP1) leads to the down-regulation of IFN-β promoter activation >24 h after poly(I:C) or virus (RSV and vesicular stomatitis virus) treatment. NAP1 is located downstream of the adapter Toll-IL-1R homology domain-containing adapter molecule (TICAM)-1 (Toll/IL-1R domain-containing adapter-inducing IFN-β) in the TLR3 pathway, but TICAM-1 and TLR3 did not participate in the IRF-3 and IFN-β promoter activation by RSV infection. Virus-mediated activation of the IFN-β promoter was largely abrogated by the gene silencing of IFN-β promoter stimulator-1 (mitochondria antiviral signaling (MAVS), VISA, Cardif), the adapter of the RIG-I/MDA5 dsRNA-recognition proteins. In both the TLR and virus-mediated IFN-inducing pathways, IκB kinase-related kinase ε and TANK-binding kinase 1 participated in IFN-β induction. Thus, RSV as well as other viruses induces replication-mediated activation of the IFN-β promoter, which is intracellularly initiated by the RIG-I/MDA5 but not the TLR3 pathway. Both the cytoplasmic and TLR3-mediated dsRNA recognition pathways converge upon NAP1 for the activation of the IRF-3 and IFN-β promoter. ***The Journal of Immunology,*** **2006, 177: 8676–8683.**

The innate immune system serves as a primary defense against virus infection (1). It is accepted that retinoic acid-inducible gene I (RIG-I)[3] recognizes dsRNA in the cytoplasm, whereas TLR3 resides in the cell membrane to engage in extracellular recognition of dsRNA (2). Human TLR3 is expressed in airway epithelial cells and macrophages/myeloid dendritic cells (mDCs), which induce cytokines, IFN type I, and chemokines in viral infection (3–5). In response to poly(I:C) or viral dsRNA, RIG-I/MDA5 (melanoma differentiation associated gene 5) as well as TLR3 have been shown to activate the transcription factor IFN regulatory factor (IRF)-3, in turn inducing the activation of the IFN-β promoter (2). It remains unsettled whether TLR3 participates in viral infection-mediated IFN-β induction by detecting the extrinsic dsRNA originating from infected cells. Some reports have suggested that influenza virus, respiratory syncytial virus (RSV), and other viruses induce TLR3-mediated cellular responses in bronchial epithelial cells (5). Cytokine/chemokine responses are reported in influenza virus and RSV infection (3, 4, 6). In particular, RSV has been reported to serve as an inefficient inducer of type I IFNs (7), thereby being in part resistant to host antiviral immunity. The identification of the two pathways initiated by TLR3 and RIG-I, which involve IRF-3 activation followed by production of IFN-β, enabled an examination of the IFN response occurring in virus-infected cells (1).

TLR3 and RIG-I act as dsRNA-recognition pattern receptors, and are followed by adapter molecules named TICAM-1 (Toll-IL-1R homology domain-containing adapter molecule 1) (Toll/IL-1R domain-containing adapter-inducing IFN-β; TRIF) and IFN-β promoter stimulator (IPS)-1 (mitochondria antiviral signaling (MAVS)/VISA/Cardif), respectively, that indirectly link the common kinase complex IκB kinase-related kinase ε (IKKε) and TANK-binding kinase 1 (TBK1) (8–14). These kinases in turn activate IRF-3 and then the IFN-β promoter (15, 16). Thus, the two pathways must converge upstream of the kinase complex. However, the primary molecule responsible for connecting the two pathways to the kinases remains undetermined. The distinctive

*Department of Microbiology and Immunology, Hokkaido University Graduate School of Medicine, Kita-ku, Sapporo, Japan; †Department of Molecular Immunology, Nara Institute for Science and Technology, Ikoma, Nara, Japan; ‡Department of Molecular Genetics, Institute for Virus Research, Kyoto University, Kyoto, Japan; and §Department of Immunology, Osaka Medical Center for Cancer, Higashinari-ku, Osaka, Japan

Received for publication May 3, 2006. Accepted for publication September 20, 2006.

The costs of publication of this article were defrayed in part by the payment of page charges. This article must therefore be hereby marked *advertisement* in accordance with 18 U.S.C. Section 1734 solely to indicate this fact.

[1] This work was supported in part by Core Research for Engineering, Science, and Technology, Japan Science and Technology Corporation, by Grants-in-Aid from the Ministry of Education, Science, and Culture (Specified Project for Advanced Research) and the Hepatitis C Virus project in National Institutes of Health of Japan, and by the Naito Memorial Foundation, Uehara Memorial Foundation, Mitsubishi Foundation, and Osaka Community Foundation. M.Sa. is supported by fellowships from the Japanese Society for the Promotion of Science.

[2] Address correspondence and reprint requests to Dr. Tsukasa Seya, Department of Microbiology and Immunology, Graduate School of Medicine, Hokkaido University, Kita-ku, Sapporo 060-8638, Japan. E-mail address: seya-tu@pop.med.hokudai.ac.jp

[3] Abbreviations used in this paper: RIG-I, retinoic acid-inducible gene I; mDC, myeloid dendritic cell; MDA5, melanoma differentiation-associated gene 5; IRF, IFN regulatory factor; RSV, respiratory syncytial virus; TICAM-1, Toll-IL-1R homology domain-containing adapter molecule 1; TRIF, Toll/IL-1R domain-containing adapter-inducing IFN-β; IPS-1, IFN-β promoter stimulator 1; MAVS, mitochondria antiviral signaling; IKKε, IκB kinase-related kinase ε; TBK1, TANK-binding kinase 1; NAP1, NAK-associated protein 1; RNAi, RNA interference; pAb, polyclonal Ab; TIRAP, Toll/IL-1R domain-containing adaptor protein; CARD, caspase activation and recruitment domain; VSV, vesicular stomatitis virus; MOI, multiplicity of infection; siRNA, small interference RNA; IRES, internal ribosome entry site; sih, small interference hairpin-loop; Q-PCR, quantitative PCR; NAP1 DN, NAP1 dominant negative.

0022-1767/06/$02.00

role of the IFN-inducing pathways in mDC also remains to be elucidated.

NAK-associated protein 1 (NAP1) is initially characterized as an activator of IKK-related kinases and suggested to be involved in protection of cells from TNF-α-induced apoptosis (17). According to the study, the virus-activated kinases IKKε and TBK1 assemble in the regulatory subunit NAP1, and NAP1 facilitates activation of NF-κB by these kinases. In contrast, NAP1 coprecipitates with TICAM-1 by immunoprecipitation, suggesting the involvement of NAP1 in the TLR3-mediated IFN-inducing pathway (18). NAP1 forms a family with IKKγ and TANK, which recruit kinases to relay the signal for cellular responses (19). We previously showed that NAP1 but not TANK interacts with TICAM-1 (18). Using the RNA interference (RNAi) technology, we have searched for a molecule linking the TLR3 TICAM-1 pathway and the virus-mediated IFN-inducing pathway by infecting HeLa or HEK293 cells with viruses (including RSV, which reportedly derives TLR3 responses; Ref. 20). The results showed the gene silencing of NAP1 and the downstream kinases, but not TLR3 or TICAM-1, led to a decrease in IFN-β promoter activation. In the same system, exogenously added poly(I:C) required both TLR3 and TICAM-1 in addition to the NAP1-kinase complex for IFN-β induction. From these studies, we conclude that NAP1 essentially participates in both the TLR3 and RIG-I/MDA5-mediated IRF-3 activation pathways.

Materials and Methods

Cell culture and HeLa cell sublines

HeLa (a human cervical carcinoma cell line) cells were cultured in MEM with 2 mM L-glutamine and 10% heat-inactivated FCS (JRH Biosciences), and its subline Hep-2 cells (Japanese Cell Resource Bank) were cultured in DMEM (Invitrogen Life Technologies) with 10% FCS and antibiotics, 100 U/ml penicillin, and 100 μg/ml streptomycin (Invitrogen Life Technologies). In some experiments, we used alternative HeLa lines with stable siNAP1 vector for NAP1 silencing or siGFP vector for control. HEK293 cells (RIKEN) were cultured in DMEM as described previously (9).

Plasmid constructs and Ab

Poly(I:C) and anti-IRF-3 Ab were purchased from Amersham Biosciences and IBL. Rabbit-polyclonal Ab (pAb) against Flag (Sigma-Aldrich), against *myc* (Santa Cruz Biotechnology), and mouse mAb against *myc* (NeoMarkers or Covance) were purchased from the indicated suppliers. A mouse mAb against human NAP1 and a rabbit pAb against human RIG-I were prepared as reported previously (2, 17). The p-125 luc reporter was a gift from Dr. T. Taniguchi (Tokyo University, Tokyo, Japan) and contained the human IFN-β promoter region (−125 to +19). The Gal4-IRF-3, Gal4-DBD, and p55 UASG-Luc for IRF-3 activation, pEF-BOS-Flag-RIG-I, RIG-IN, MDA5, and MDA5N were described in Refs. 21 and 22). Expression vectors for NAP1-full, NAP1-DN, and del-NAP1 (NAP1 deleted of the TBK1 binding site; 158–270 aa) in pcDNA3.1 were prepared as described previously (17). Expression vector for IPS-1 (pEF-BOS-Flag-IPS1) was amplified by PCR using KIAA1271 (Kazusa DNA Research Institute) as a template. The dominant-negative form of Mal (Toll/IL-1R domain-containing adaptor protein; TIRAP) was prepared as described previously (23).

Immunoprecipitation

Methods for immunoprecipitation and immunoblotting were described previously (23). Briefly, HEK293 cells were transiently transfected with expression vectors in a 6-well plate using LipofectAMINE 2000 reagent (Invitrogen Life Technologies) and allowed to stand for 24 h. Cells were lysed and proteins were immunoprecipitated with anti-*myc* mAb (NeoMarkers). Immunoprecipitants were washed, resolved on SDS-PAGE (7.5 or 10% gel), and visualized by immunoblotting using the anti-Flag pAb or anti-*myc* pAb.

HeLa cells were used for detection of the endogenous NAP1-RIG-I interaction. Cells were cultured in DMEM/10% FCS with or without recombinant human IFN-β (1000 IU/ml) for 24 h. Cell lysates were immunoprecipitated by anti-NAP1 mAb or anti-mouse IgG Ab. Coimmunoprecipitation was detected by anti-RIG-I pAb.

Reporter gene assay

Activation of the IFN-β promoter was measured by reporter assay. HEK293 cells were transfected in 24-well plates using LipofectAMINE 2000 reagent with a p-125 luc (IFN-β) reporter plasmid together with the RIG-I, RIG-IN, MDA5, MDA5N or IPS-1, and NAP1 158–270 (NAP1-DN) plasmids. The properties of RIG-IN and MDA5N were published in a previous study (22). Briefly, the caspase activation and recruitment domain (CARD) of RIG-I (aa 1–284) acted as a constitutive active nature in the IFN-β induction. Luciferase activity was measured by the Dual-Luciferase assay kit (Promega). The luciferase activity of firefly was normalized to that of *Renilla*, and relative activation was determined. All experiments were performed in triplicate. Data were expressed as the means ± SD.

Assay for IRF-3 activation

Two methods, reporter assay (21) and native gel assay (24), were used to determine the degree of IRF-3 activation. In some experiments, cells were stimulated with medium alone, poly(I:C) (10 μg/ml), or vesicular stomatitis virus (VSV). In some experiments of reporter assay, cells were transfected with poly(I:C) using DEAE-dextran at 24 h posttransfection. Six hours later, cells were harvested to measure the expression of luciferase using the dual luciferase assay kit (Promega). Data were expressed as the means ± SD. In native assay, cells were lysed after 8 h VSV infection (multiplicity of infection (MOI) = 10). The protein level of each sample was measured by the Protein assay Kit (Bio-Rad) and normalized 20 μg/each lane. Extracts were separated on 7.5% native gel and immunoblotting with anti-IRF-3 Ab (24).

Confocal microscope analysis

HeLa cells (1.5×10^5 cells/well) were plated onto coverslips in a 24-well plate. After cells adhered onto coverslips, cells were transiently transfected with Flag-tagged IPS-1, *myc*-tagged NAP1, and/or *myc*-tagged TANK using LipofectAMINE reagent (Invitrogen Life Technologies). Twenty-four hours later, in a typical experiment, cells were treated with 250 nM Mito Tracker Red (Molecular Probes) for 1 h. Cells on coverslips were washed twice with PBS and fixed in 3% formaldehyde in PBS for 30 min. Cells were permeabilized with staining buffer (3% BSA in PBS) containing 0.5% saponin for 30 min at room temperature. After three washes with staining buffer, cells were incubated with primary Ab diluted in staining buffer for 1 h. Cells were extensively washed, and then were treated with Alexa Fluor 488 monoclonal or polyclonal, or Alexa Fluor 594 pAbs (Molecular Probes) as secondary Ab for 30 min. After three washes, coverslips with the cells were mounted onto slide glasses using 2.3% DABCO in PBS. Imaging of the cells was curried out using Olympus Fluoview laser scanning confocal microscopy (25).

Virus preparation and infection

Human RSV field-isolate strain (RSV2177) in subgroup B was propagated with Hep-2 cells (provided by Dr. K. Imai, Wakayama Prefectural Center, Wakayama, Japan) (26). The titer of RSV2177 was determined by 50% tissue culture infective dose using Hep-2 cells. This RSV strain derives type I IFN from Hep-2 cells >24 h postinfection (M. Shingai and T. Seya, unpublished observation). HeLa cells were infected with RSV for small interference RNA (siRNA) knockdown studies at MOI = 1 or 2.5.

VSV was propagated as described previously (27). In brief, VSV (Indiana strain) was propagated with L929 cells. The titration of VSV was determined by plaque assay using L929 cells. HeLa cells were infected with VSV at MOI = 10.

RNAi

RNAi knockdown by siRNA-containing vectors was performed regarding NAP1 as follows. A DsRed2 fragment derived from pDsRed2 (BD Clontech) was cloned into pBluescript II (Stratagene). To paste into the *Xho*I and *Spe*I site of the vector, the *Pst*I site of DsRed2 was replaced with CTGCAA by site-directed mutagenesis. Internal ribosome entry site (IRES) and puromycin resistance gene (Puro) fragments were amplified with an Expand High Fidelity PCR system (Roche Diagnostics) by using the following primer sets: AAACTAGTGCCCCTCTCCCTCCC and CTCACCATGGTTGTGGCCATATTATCATCGTGTTTTTCAAA, and AAACTCGAGTCCACCATGGGCACCGAGTACAAGCCC ACGGT and AAAACTAGTGCGGCCGCTCAGGCACCGGGCTT GCGGG, respectively. pME-Puro vector was generated by cloning of the *Xho*I-*Spe*I fragment of Puro and placing it between the *Xho*I and *Xba*I sites of the pME vector. The *Xho*I-*Spe*I fragment of DsRed2 and the *Spe*I-*Nco*I fragment of IRES were cloned into the pME-Puro vector. pH1′ vector was a gift from Drs. H. Hasuwa and M. Okabe (Osaka, Japan) (28). pH1′-DsRed-IRES-Puro was constructed by subcloning of

Table I. *Primer sets*

	Primer Set for RT-PCR	
	Forward	Reverse
RIG-I	5′-GATGGCAGGTGCAGAGAAA-3′	5′-GGAGTTAAAATGATGATGTC-3′
MDA5	5′-TCCAACTGCTGAACCTCCT-3′	5′-TGCCCATGTTGCTGTTATGT-3′
IPS-1	5′-TGCCGTTTGCTGAAGACAA-3′	5′-TTCGTCCGCGAGATCAACT-3′
	Primer Set for Q-PCR	
	Forward	Reverse
IFN-β	5′-CAACTTGCTTGGATTCCTACAAAG-3′	5′-TATTCAAGCCTCCCATTCAATTG-3′
β-Actin	5′-CCTGGCACCCAGCACAAT-3′	5′-GCCGATCCACACGGAGTACT-3′

the *Hin*dIII-*Kpn*I fragment of the pME-DsRed2-IRES-Puro vector into the pH1′ vector. Oligonucleotides were cloned into pH1 vector to express small interference hairpin-loop (sih)GFP and sihNAP1 (two sites) hairpins downstream of the human H1 RNA promoter as described previously (18, 28). 5′-AAGCTAATAGCTCGATTT-GAAGA-3′ and 5′-AAGTGATAATATGCAGCATGCAT-3′ were the sequences targeted for sihNAP1-A and sihNAP1-B, respectively. The target sequence for sihGFP has been described earlier (28).

HeLa cells were transfected with pH1-GFP, pH1-NAP1-A, or pH1-NAP1-B (100 nM/4 × 10^5 cells) using PolyFect (Qiagen). Bulk cell populations in 1 mg/ml puromycin were selected from which single colonies were picked up for further analysis. To determine the efficiency of gene silencing, total RNA from each clone was isolated with RNeasy (Qiagen) and mRNA was estimated by RT-PCR. The primers used for PCR were GAPDH primers, and NAP1-F and NAP1-R for NAP1 (18).

The method for gene silencing using siRNA oligonucleotides was described previously (23). The sequences of the siRNA for TICAM-1 (9), TBK1, IKKε (15), RIG-I, and IPS-1 (MAVS) were reported previously (14). The target sequence for human MDA5 gene silencing is 5′-AAAUACCAUAAUGGAGCAAUA-3′. Knockdown was analyzed by RT-PCR.

Detection of human IFN-β mRNA

RT-PCR and quantitative PCR (Q-PCR) were performed as described previously (23). Briefly, human cells were transfected with gene silencing or dominant-negative-expressing vectors (100 nM/4 × 10^5 cells) 24 h before infection. Cells were then infected with RSV (MOI = 1–2.5). Twenty-four hours later, total RNA was extracted from cells with RNeasy mini kit (Qiagen) and cDNA was generated by M-MLV-reverse transcriptase

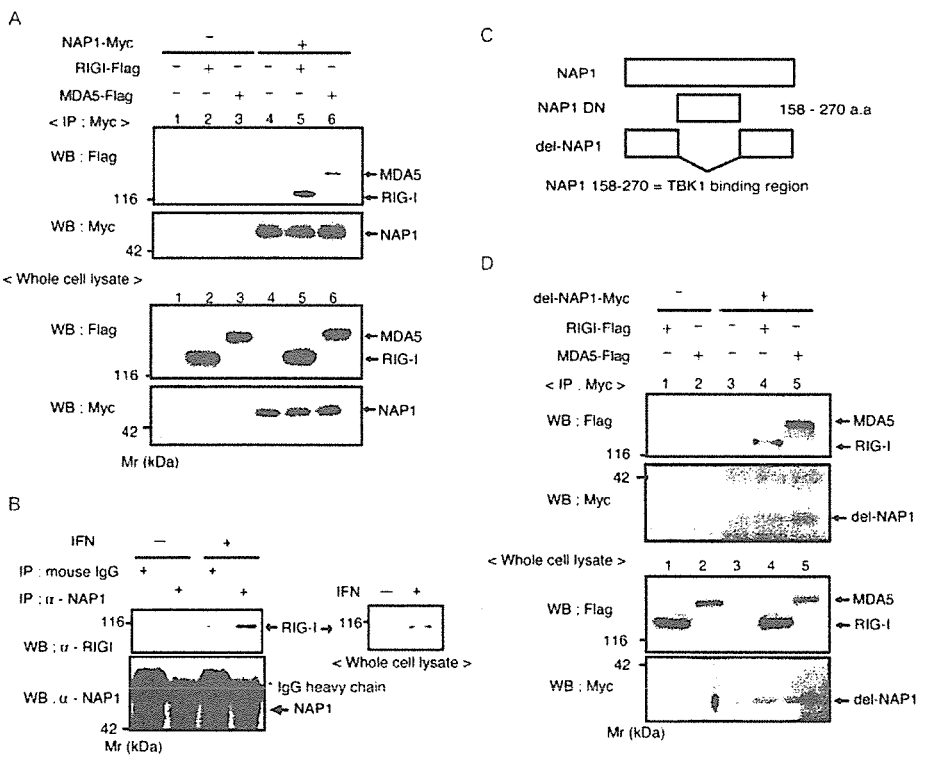

FIGURE 1. NAP1 interacts with RIG-I and MDA5. *A* and *D*, NAP1 associated with RIG-I and MDA5 in overexpression system. HEK293 cells were transiently transfected with expression vectors of NAP1 (*A*) or del-NAP1 (*D*) (*myc*-tagged), together with RIG-I or MDA5 (Flag-tagged) or empty vector, and allowed to stand for 24 h. Cells were then lysed and the lysates immunoprecipitated with anti-*myc* Ab. The precipitates were resolved on SDS-PAGE and transferred onto membrane. The blot was probed with anti-*myc* or anti-Flag Ab. Arrows indicate the positions of NAP1, RIG-I, and MDA5. M_r markers are shown to the *left*. *B*, Endogenous interaction between NAP1 and RIG-I. HeLa cells were pretreated with recombinant human IFN-β for 24 h. Extracts from IFN-treated or nontreated HeLa cells were immunoprecipitated with indicated Ab. The blot was probed with anti-RIG-I pAb or anti-NAP1 mAb. *, Indicates the mouse Ig H chain and arrow indicates the NAP1 or RIG-I band. Data are representative of three (*A* and *D*) or two (*B*) independent experiments. *C*, A schematic diagram of NAP1. The region of NAP1 158 to 270 aa was directly associated with TBK1.

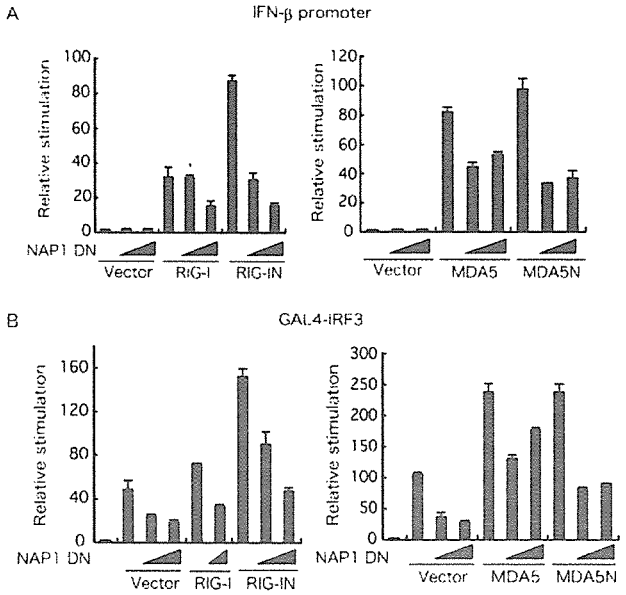

FIGURE 2. NAP1 participates in IRF-3, NF-κB, and IFN-β promoter activation via RIG-I and MDA5. *A*, HEK293 cells were transfected with the dominant-negative form of NAP1 158–270 (NAP1 DN) and expression vector RIG-I, RIG-IN (*left panel*), MDA5 or MDA5N together with the IFN-β promoter reporter plasmids. *B*, HEK293 cells were transiently transfected with p55-UAS$_G$Luc and pEF-GAL4/IRF-3, NAP1 DN, and empty vector, together with RIG-I, RIG-IN (*left panel*), MDA5 or MDA5N (*right panel*). After 24 h, luciferase reporter activity was measured and the relative firefly luciferase activity shown in normalized by *Renilla* luciferase activity. All data are representative of three independent experiments.

(Promega). cDNA was subjected to PCR using Ex-*Taq* DNA polymerase (Takara). For this study, previously described primer sets for IFN-β, NAP1, and TICAM-1 for silencing, and GAPDH or β-actin for internal control were used (9, 18, 23). Other primer sets for TBK1, IKKε, RIG-I, MDA5, and IPS-1 were described in Table I. Q-PCR was performed with iQ SYBER Green Super mix and iCycler iQ real-time PCR analyzing system (Bio-Rad). The primers used for IFN-β and β-actin on the Q-PCR were described in Table I. The copy number of IFN-β mRNA was normalized to β-actin mRNA, and relative fold induction of the medium to control was determined.

Results

NAP1 binds RIG-I and MDA5 in HEK293 transfectants

First, we tested whether RIG-I coprecipitates with NAP1 by immunoblotting using HEK293 cells. Cells were transfected with the indicated plasmids (Fig. 1*A*) and 24 h later solubilized with Nonidet P-40. NAP1 was immunoprecipitated with anti-*myc* Ab. Anti-Flag or anti-*myc* Ab was used as a probe for protein detection in immunoblotting. Flag-tagged RIG-I was shown to form a complex with *myc*-tagged NAP1 by analysis with SDS-PAGE followed by immunoblotting. RIG-I was identified together with NAP1 on the sheet, suggesting that RIG-I physically binds NAP1. Similar results were obtained with NAP1 and MDA5 (Fig. 1*A*). To confirm endogenous RIG-I physically binds NAP1, we used HeLa cells pretreated with IFN-β (Fig. 1*B*). RIG-I was efficiently induced in HeLa cells 24 h after IFN treatment (*inset* of Fig. 1*B*) and pulled down with NAP1 by immunoprecipitation using the mAb against NAP1.

NAP1 (158–270) (NAP1 DN; NAP1 dominant negative) can directly bind TBK1 and serve as a dominant-negative form in TICAM-1-mediated IFN signaling (17, 18). We tested whether NAP1 deleted this region (158–270) (del-NAP1) (Fig. 1*C*) could still interact with RIG-I and MDA5. Del-NAP1 preserves the ability to bind RIG-I and MDA5. Both RIG-I and MDA5 coprecipitated with this NAP deletion mutant (Fig. 1*D*), suggesting that the RIG-I/MDA5 binding site is mapped outside the TBK1 binding site. Because the large amount of NAP1 present in human cells prevents overexpression analysis, NAP1 DN was used for the following experiments as a dominant negative for the IFN pathway.

RIG-I and MDA5 participate in the NAP1-mediated signaling

RIG-I and MDA5 contain two CARDs. The CARDs of RIG-I recruits a CARD-containing adapter IPS-1. The CARD domains of RIG-I (RIG-IN) and MDA5 (MDA5N) have been used in addition

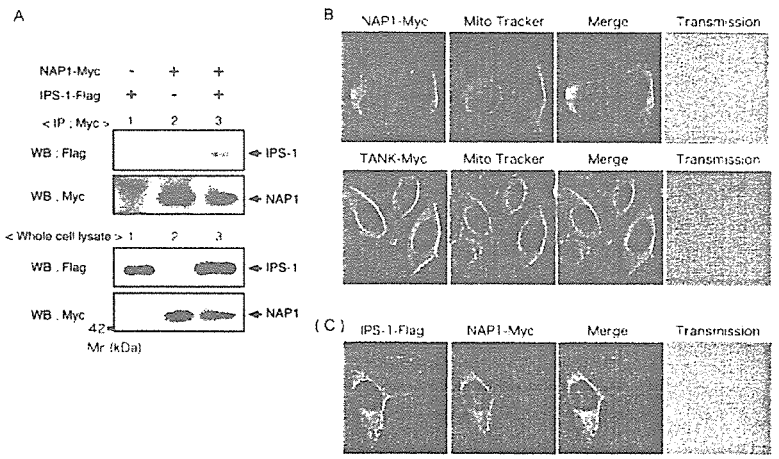

FIGURE 3. NAP1 colocalizes with IPS-1 in mitochondria. *A*, Minute physical interaction between NAP1 and IPS-1. HEK293 cells were transfected with *myc*-tagged NAP1 and flag-tagged IPS-1. After 24 h of transfection, cell extracts were immunoprecipitated by anti-*myc* mAb. The precipitates were resolved on SDS-PAGE and transferred onto membrane. The blot was probed with anti-*myc* or anti-Flag Ab. Arrows indicate the positions of NAP1 and IPS-1. M_r markers are shown to the *left*. *B*, NAP1 partially located around mitochondria. HeLa cells onto coverslips were transfected with NAP1 or TANK (*myc*-tagged). Twenty-four hours after transfection, cells were incubated with Mito Tracker Red for 1 h. *myc*-tagged NAP1 or TANK were stained with anti-*myc* mAb and imaged by confocal microscopy. The yellow staining in the overlay indicates colocalization of NAP1 and Mito Tracker. *C*, NAP1 colocalized with IPS-1. HeLa cells onto coverslips were transfected with IPS-1 (Flag-tagged) and NAP1 (*myc*-tagged). Twenty-four hours after transfection, cells were stained with anti-*myc* mAb and anti-Flag pAb and imaged by confocal microscopy. Data are representative of four (*A*) or three (*B*) independent experiments.

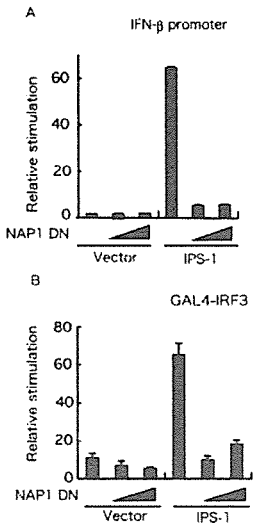

FIGURE 4. NAP1 DN-interfered IFN-β promoter and IRF-3 activation by IPS-1. *A*, HEK293 cells were transfected with the NAP1 DN and expression vector for IPS-1 together with the IFN-β promoter reporter plasmids. Cells were analyzed 24 h after transfection for promoter activity by a reporter gene assay. *B*, HEK293 cells were transiently transfected with p55-UAS$_G$Luc and pEF-GAL4/IRF3 and NAP1 DN together with empty vector or expression vector for IPS-1. Twenty-four hours after transfection, cells were collected and the promoter activation was measured by reporter gene assay. All data are representative of three independent experiments.

to RIG-I and MDA5 for signaling studies. IFN promoter was activated in cells expressing RIG-IN and to a lesser extent in cells with full-length RIG-I (Fig. 2*A*). In this context, MDA5 and MDA5N elicited comparable activities. When increasing doses of NAP1 DN were added to the cells with RIG-I, MDA5, or their mutants, IFN-β promoter activation was prohibited by NAP1 DN

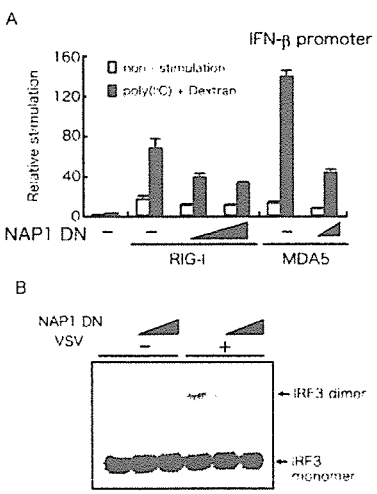

FIGURE 5. NAP1 DN inhibits IRF-3 activation. *A*, HEK293 cells were transfected with IFN-β promoter reporter plasmid together with the plasmids of RIG-I or MDA5 (100 ng) and NAP1 DN. Twenty-four hours after transfection, cells were transfected with dextran-only (nonstimulated) or poly(I:C)-mixed dextran for 6 h. *B*, HEK293 cells were transfected with NAP1 DN and cultured for 24 h. Cells were infected with VSV (MOI = 10) for 8 h. Extracts were subjected to native PAGE according to the reported method. Relative signal intensities of the dimer are shown below the lanes. These data are representative of three (*A*) or two (*B*) independent experiments.

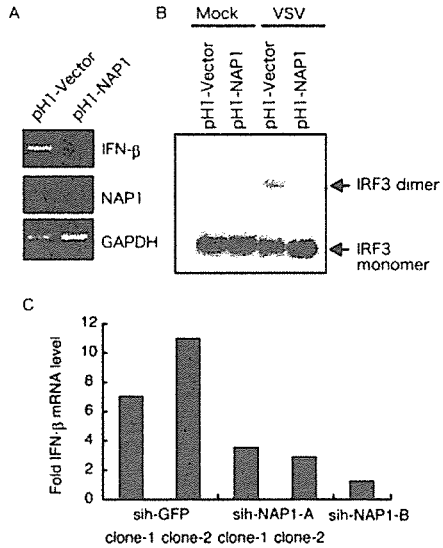

FIGURE 6. Implication of NAP1 in VSV infection-mediated IFN-β induction. *A*, NAP1 stable knockdown HeLa cells generate low levels of IFN-β mRNA in VSV infection. HeLa clones with the stably silencing NAP1 gene (data shown for pH1-NAP-A clone-1) or empty vector (control) were infected with VSV (MOI = 10) for 12 h. Total RNA was prepared, and RT-PCR analysis was performed with specific primers for NAP1, IFN-β, and GAPDH. *B*, NAP1-mediated IRF-3 activation in VSV infection. Stable NAP1-silenced HeLa cells (5.0×10^5 cells, pH1-NAP1-A clone-1) were infected with VSV (MOI = 10) for 8 h. Extracts were resolved by native gel electrophoresis. Dimerization of IRF-3 was detected by immunoblotting. *C*, VSV-mediated IFN-β induction is suppressed by NAP1 gene silencing. HeLa clones stably depleting NAP1 (clone-1 and clone-2 for sih-NAP1-A and a clone for sih-NAP1-B) or expressing siRNA against GFP (sih-GFP clone-1 and clone-2) were infected with VSV (MOI = 10) for 12 h. The IFN-β mRNA levels were determined with these cells by Q-PCR. Data are representative of two (*B*) or three (*C*) independent experiments.

in a dose-dependent manner (Fig. 2*A*). Using the Gal4-IRF-3 activation system, RIG-I- and MDA5-mediated IRF-3 activation was impaired in cells expressing NAP1 DN dose dependently (Fig. 2*B*). In the two systems, RIG-IN more potentially activated the promoters than intact RIG-I, whereas MDA5 and MDA5N exhibited similar tendencies (Fig. 2). Thus, the CARD domain of RIG-I induces activation of IRF-3 and IFN-β promoter, both of which are regulated by NAP1. It is notable, although consistent with a previous report (22), that the full-length MDA5 that contains the helicase domain exhibited high IFN-inducing activity compared with the case of RIG-I. A functional link between RIG-I/MDA5 and NAP1 is confirmed by this analysis in addition to the physical linkage.

Physical association between NAP1 and IPS-1

We next examined the ability of NAP1 to recruit IPS-1 in HEK293 cell transfectants. By simple immunoprecipitation analysis, NAP1 managed to coprecipitate with IPS-1 (Fig. 3*A*). Because IPS-1 resides in the mitochondrial membrane (14), we homogenized the transfectants and collected the mitochondria-rich fraction. Similar blotting results were obtained using this fraction (data not shown). Because NAP1 is a cytoplasmic protein, we investigated the localization of NAP1 using *myc*-tagged NAP1 expressed in HeLa cells by confocal microscopy. NAP1 was distributed in cytoplasm, particularly located around mitochondria (Fig. 3*B*, *upper panel*). In contrast, TANK, which is a structural homologue of NAP1, barely merged with mitochondrial marker (Fig. 3*B*, *lower panel*). To test